Effects of relativity in proton-proton bremsstrahlung

G. H. Martinus and O. Scholten
Kernfysisch Versneller Instituut, 9747 AA Groningen, the Netherlands

J. A. Tjon
Institute for Theoretical Physics, University of Utrecht, 3508 TA Utrecht, the Netherlands
(Received 3 July 1997)

We investigate the influence of negative-energy states in proton-proton bremsstrahlung in a fully relativistic framework using the T matrix of Fleischer and Tjon. The contribution from negative-energy states in the single-scattering diagrams is shown to be large, indicating that relativistic effects are important. The rescattering contribution compensates some of the effect, which is shown to be a consequence of a low-energy theorem. The net effect of negative-energy states nevertheless is of the order of 20% at higher energies. We investigate retardation effects in the nucleon-nucleon (NN) interaction by means of a one-pion exchange model, which gives effects of the order of 15% at the pion-production threshold. We furthermore modify the NN T matrix to incorporate some of these effects, and find that on the level of single-scattering contributions they are of the order of 10%. We show predictions at incoming proton energy $T_{\text{lab}}=190$ MeV, where high accuracy measurements are being done at KVI, and conclude that even at these relatively low energies off-shell effects in the NN interaction and contributions from negative-energy states clearly show up. [S0556-2813(97)00811-X]

PACS number(s): 13.75.Cs, 21.45.+v, 24.10.Jv, 25.20.Lj

I. INTRODUCTION

Proton-proton bremsstrahlung is one of the simplest processes involving the half off-shell nucleon-nucleon (NN) interaction. Since protons are equally charged particles, electric-dipole radiation is suppressed and higher-order effects play an important role. Thus it is possible to get information on the NN force not easily obtained from other processes. Proton-proton bremsstrahlung has the additional advantage that meson-exchange currents, necessary for current conservation in the proton-neutron case, are suppressed. Therefore other higher-order effects, such as the contribution from intermediate Δ's [1] or negative-energy states (pair currents), can become important. In this paper we will concentrate on the influence of relativistic effects such as the role of negative-energy states.

A relativistic model is used that includes these states in a dynamical way. We find that including negative-energy states gives substantial effects in both the cross section and the analyzing power. As compared to recent work by Eden and Gari [2] who use a Hamiltonian formalism, and of de Jong and Nakayama [3] who used the NN T matrix of a relativistic spectator model [4], the relativistic contributions are in general found to be more enhanced, especially in the cross-section predictions. The effects are of the order of 20% in the cross section for forward and backward photon angles and small proton angles at energies close to the pion-production threshold (i.e., large photon momenta).

The outline of the article is as follows. First we will present the relativistic framework in which the NN interaction is generated, and in Sec. III we will describe how this interaction can be applied to describe the bremsstrahlung process. In Sec. IV we discuss the importance of negative-energy states in the present framework, and compare to other calculations that include these intermediate states. We show that the partial cancellation of the contributions of negative-energy states from the single-scattering diagrams by those from the rescattering diagram can be understood on the basis of the low-energy theorem for proton-proton bremsstrahlung. This strong suppression of the effect of negative-energy states is in sharp contrast with the case of Compton scattering, where negative-energy states give the major contribution to the full matrix element. We discuss the influence of retardation in the NN interaction, and show that this gives rise to effects of the order of 10% in the cross section calculated in impulse approximation at pion production threshold.

A comparison to the existing data just below the pion-production threshold ($T_{\text{lab}}=280$ MeV) from the TRIUMF experiment [5] is made in Sec. V, where we furthermore present our predictions at $T_{\text{lab}}=500$ MeV and for the kinematics as is being carried out at KVI [6] at $T_{\text{lab}}=190$ MeV. It is shown that the effects increase with the energy, as is to be expected, but that even for the data at the relatively low energy of 190 MeV relativistic effects are important. Finally in Sec. VI some concluding remarks are made.

II. NN INTERACTION

In this section we will briefly summarize the field-theoretical Bethe-Salpeter (BS) equation for the two-proton interacting system and the quasipotential approximation to it. The nuclear interaction is based on a one-boson exchange (OBE) model with only nucleonic and mesonic degrees of freedom.

Within the relativistic field theory two particle scattering is described by the scattering T matrix. This T matrix $T(p,p';P)$ is a solution of the inhomogeneous BS equation,

$$T(p,p';P)=V(p,p') -i\int \frac{d^4k}{(2\pi)^4}V(p,k)S_2(k,P)T(k,p',P), \tag{1}$$

where $S_2(p,P)=S^{(1)}(p,P)S^{(2)}(p,P)$ and $S^{(i)}$ are the free one-particle propagators of the two nucleons with relative momentum p and total momentum P. In our case the NN interaction $V(p,p')$ is assumed to be given by the one-boson exchange model of Fleischer and Tjon [8,9]. In this OBE model the interaction is described by the exchange of π, ρ, ω, η, ϵ (or σ) and δ mesons.

The contributions from the isovector mesons π, ρ, and δ to the interaction are given by

$$\begin{aligned}
V_\pi(k,p)&=-i\frac{g_\pi^2}{4M^2}(\gamma_5(\not k-\not p))^{(1)}\Delta_\pi(k-p)\\
&\quad\times(\gamma_5(\not k-\not p))^{(2)}\tau_1\cdot\tau_2,\\
V_\rho(k,p)&=-ig_\rho^{\mathrm{v}2}\left(\gamma_\alpha^{(1)}-\frac{ig_\rho^{\mathrm{T}}}{2M}\sigma_{\alpha\mu}^{(1)}(k-p)^\mu\right)\Delta_\rho^{\alpha\beta}(k-p)\\
&\quad\times\left(\gamma_\beta^{(2)}+\frac{ig_\rho^{\mathrm{T}}}{2M}\sigma_{\beta\nu}^{(2)}(k-p)^\nu\right)\tau_1\cdot\tau_2,\\
V_\delta(k,p)&=-ig_\delta^2\Delta_\delta(k-p)\tau_1\cdot\tau_2,
\end{aligned} \tag{2}$$

which are, respectively, of the pseudovector, vector, and scalar type. The ω, ϵ, and η mesons give the isoscalar contributions to the interaction, which are of the form

$$\begin{aligned}
V_\omega(k,p)&=-ig_\omega^{\mathrm{v}2}\gamma_\alpha^{(1)}\Delta_\omega^{\alpha\beta}(k-p)\gamma_\beta^{(2)},\\
V_\epsilon(k,p)&=-ig_\epsilon^2\Delta_\epsilon(k-p),\\
V_\eta(k,p)&=-i\frac{g_\eta^2}{4M^2}(\gamma_5(\not k-\not p))^{(1)}\Delta_\eta(k-p)(\gamma_5(\not k-\not p))^{(2)},
\end{aligned} \tag{3}$$

which are of the vector, scalar, and pseudovector type, respectively. The bracketed numbers in both defining equations denote the nucleon on which the matrices γ_μ and $\sigma_{\mu\nu}$ act. The propagators Δ_μ for the pseudoscalar (π and η) and scalar (δ and ϵ) mesons is

$$\Delta(p)=\frac{1}{m^2-p^2}, \tag{4}$$

whereas the propagator $\Delta^{\mu\nu}$ for the vector mesons ρ, ω is given by

$$\Delta^{\mu\nu}(p)=\left(-g^{\mu\nu}+\frac{p^\mu p^\nu}{m^2}\right)\frac{1}{m^2-p^2} \tag{5}$$

with m the mass of the meson.

With the OBE exchange as defined in Eqs. (2) and (3) the integrations in the BS equation do not converge. To ensure the correct behavior for high momenta a phenomenological cutoff is introduced of the monopole form,

$$F(p^2)=\frac{\Lambda^2}{\Lambda^2-p^2}, \tag{6}$$

at each meson-nucleon vertex, with Λ being the cutoff mass. In this OBE model the cutoff masses are taken to be the same for all mesons.

In principle, the full field-theoretical Bethe-Salpeter equation can be solved [10]. However, the calculations are highly nontrivial and in practice usually a quasipotential approximation is made. In the quasipotential framework the two-particle propagator is replaced by one where the relative energy variable is restricted in such a way that properties like two-particle unitarity and relativistic covariance are maintained. Several approximations have been studied in the literature (for a review see Ref. [11]). Here we choose the approximation in which the two nucleons are treated in a symmetrical way, the Blankenbecler-Sugar-Logunov-Tavkhelidze (BSLT) approximation [12]. The scalar part of the two-nucleon propagator,

$$G_0=\frac{1}{\left(\frac{1}{2}P+p\right)^2-M^2+i\epsilon}\,\frac{1}{\left(\frac{1}{2}P-p\right)^2-M^2+i\epsilon}, \tag{7}$$

is replaced by the dispersion relation

$$G_2^{\mathrm{BSLT}}=\int_{4M^2}^{\infty}ds'\,\frac{f(\sqrt{s'},\sqrt{s})}{s'-s}\,\mathrm{Disc}(G_0), \tag{8}$$

where s is the total invariant energy $s=P^2$ and the discontinuity of G_0 is taken to be

$$\begin{aligned}
\mathrm{Disc}(G_0)&=i\pi\delta^+\left[\left(\sqrt{\frac{s'}{s}}\frac{P}{2}+p\right)^2-M^2\right]\\
&\quad\times\delta^+\left[\left(\sqrt{\frac{s'}{s}}\frac{P}{2}-p\right)^2-M^2\right].
\end{aligned} \tag{9}$$

The function f can be arbitrary, apart from that it has to be free of singularities in the physical region and is constrained by $f(\sqrt{s},\sqrt{s})=1$. The definition in the form of a dispersion relation guarantees that G_2^{BSLT} has the same discontinuity as G_0. Consequently two-particle unitarity is preserved. Thus we assume implicitly that inelastic processes, which are, in principle, included in the full BS equation for energies beyond the pion-production threshold, are not important and can be neglected.

We may now use the freedom of f to regulate the two-nucleon propagator for large momenta. Choosing

$$f(\sqrt{s'},\sqrt{s})=\frac{2\sqrt{s'}}{\sqrt{s'}+\sqrt{s}}, \tag{10}$$

we get in the center-of-mass frame of the two-particle system

$$G_2^{\mathrm{BSLT}}=i\pi\frac{1}{E_p-E}\,\frac{1}{(E_p+E)^2}\,\delta(p_0), \tag{11}$$

where $E=\frac{1}{2}P_0$ and $E_p=\sqrt{p^2+M^2}$. Then the full two-nucleon propagator, including the spinor structure, is given by

TABLE I. The coupling parameters for the various fits. Fit A corresponds to the parameters used in Ref. [8]. In all fits we have $g_\pi^2/4\pi=14.2$, $g_\rho^V/4\pi^2=0.43$, $g_\rho^T/g_\rho^V=6.8$, $g_\omega^2/4\pi=11.0$, and $g_\eta^2/4\pi=3.09$, while the cutoff mass is $\Lambda^2=1.5M^2$.

Fit	$g_\epsilon^2/4\pi$	$g_\delta^2/4\pi$
A	7.34	0.33
B	7.60	0.75
C	7.30	0.55

$$
\begin{aligned}
S_2^{\mathrm{BSLT}}(p,P) &= \frac{1}{2\pi i}\left(\frac{1}{2}\not{P}+\not{p}+M\right)^{(1)}\left(\frac{1}{2}\not{P}+\not{p}+M\right)^{(2)} G_2^{\mathrm{BSLT}} \\
&= \frac{1}{2\pi i}[(E+E_p)\Lambda_+^{(1)}+(E-E_p)\Lambda_-^{(1)}] \\
&\quad \times[(E+E_p)\Lambda_+^{(2)}+(E-E_p)\Lambda_-^{(2)}]G_2^{\mathrm{BSLT}} \\
&= \frac{1}{2}(E_p-E)\,\delta(p_0)S^{(1)}(p,P)S^{(2)}(p,P), \qquad (12)
\end{aligned}
$$

where the projection operators $\Lambda_\pm^{(i)}$ are defined in Appendix A. In particular, with this choice we get for the two-nucleon propagator in the positive energy spinor states

$$
S_{++}=\frac{1}{2}\frac{1}{E_p-E}. \qquad (13)
$$

Using Eq. (12) for the two-nucleon propagator, the integration over the relative energy p_0 in the inhomogeneous BS equation can be performed, and the BSLT equation is obtained,

$$
\begin{aligned}
T(\hat{p},\hat{p}';P) &= V(\hat{p},\hat{p}')+\frac{1}{(2\pi)^3} \\
&\quad \times\int d^3k V(\hat{p},\hat{k})S_2^{\mathrm{BSLT}}(\hat{k},P)T(\hat{k},\hat{p}',P),
\end{aligned} \qquad (14)
$$

where $\hat{p}$, $\hat{p}'$, and $\hat{k}$ are the relative four-momenta p, p', and k under the restriction that in the c.m. system of the nucleons the energy component is zero, $p_0=0$, $p_0'=0$, and $k_0=0$.

The BSLT equation can be solved in a partial-wave basis [13], yielding a number of coupled-channel equations, that involve essentially a coupled set of one-dimensional integral equations due to the quasipotential approximation. Aside from the physical $(+,+)$ positive-energy states, also combinations involving negative-energy states occur $[(-,-)$, and even and odd combinations of $(+,-)$ and $(-,+)]$. The T matrix has been fitted to the experimental phase shifts of Arndt *et al.* [14] by varying the meson-nucleon coupling constants. Fits have been made both with and without intermediate negative-energy states for energies up to 200 MeV. Starting from the found fit with the full Dirac structure included, we simply have only varied the coupling constants g_ϵ and g_δ to obtain a fit for the case of the absence of intermediate negative states. The sets of the coupling parameters for the different fits are given in Table I and the corresponding caption. The resulting phase shifts for both fits can be considered almost phase equivalent and are up to 300 MeV in reasonable agreement with the Arndt phases.

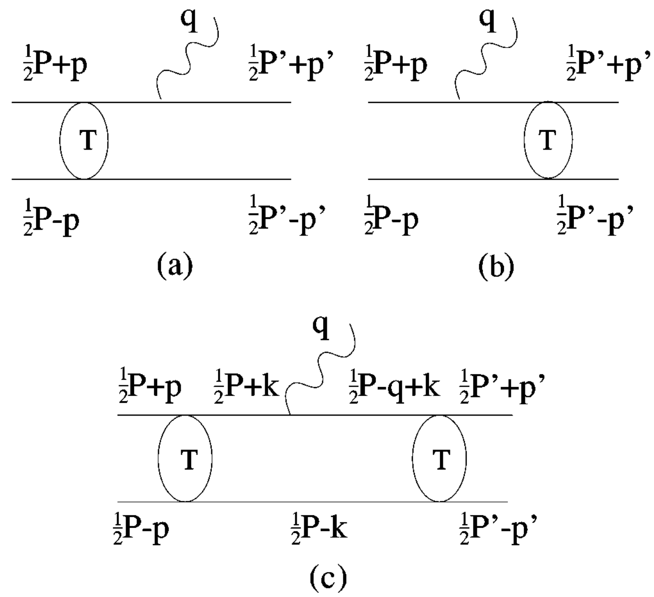

FIG. 1. The diagrams taken into account in the present calculation. Diagrams (a) and (b) are the single-scattering contributions, the sum of which is the impulse approximation (IA). Diagram (c) is the rescattering contribution.

III. THE BREMSSTRAHLUNG AMPLITUDE

The dynamics of the bremsstrahlung process is contained in the invariant matrix, $M_{fi}=\varepsilon^\mu\langle f|J_\mu|i\rangle$ with ε^μ the photon polarization vector. If the T matrix is properly antisymmetrized, the nuclear current J_μ is given by

$$
\begin{aligned}
\langle f|J_\mu|i\rangle &= \langle p',P'|T(p',\tilde{p};P')S^{(1)}(\tilde{p},P')\Gamma_\mu^{(1)}(q)|p,P\rangle \\
&\quad +\langle p',P'|\Gamma_\mu^{(1)}(q)S^{(1)}(\tilde{p}',P)T(\hat{p}',p;P)|p,P\rangle \\
&\quad +(1\leftrightarrow 2)-i\int\frac{d^4k}{(2\pi)^4}\langle p',P'|[T(p',k';P')S^{(1)} \\
&\quad \times(k',P')\Gamma_\mu^{(1)}(q)S_2(k,P)T(k,p;P)]|p,P\rangle. \qquad (15)
\end{aligned}
$$

The sum of the first two terms will be referred to as the impulse approximation (IA). The corresponding diagrams are shown in Figs. 1(a) and 1(b). The last term is referred to as the rescattering contribution, corresponding to the diagram in Fig. 1(c). Using the antisymmetry of the protons the diagram where the photon is emitted by intermediate particle 2 can be rewritten as a diagram where the photon is emitted by particle 1, and if the T matrix is antisymmetrized the antisymmetrized sum of all rescattering diagrams can be shown to be given by the diagram with antisymmetrized T matrices with emission from particle 1 only. The momenta in Eq. (15) are defined through conservation of four momentum at the NNγ vertex and of total momentum, so that $p'=p-\frac{1}{2}q$ and $P'=P-\frac{1}{2}q$.

In Eq. (15) the electro-magnetic (e.m.) vertex Γ_μ is taken to be the on-shell form

$$\Gamma_\mu^{(i)}(q)=e\left(F_1^{(i)}(q^2)\gamma_\mu^{(i)}-\frac{i}{2M}F_2^{(i)}(q^2)\sigma_{\mu\nu}^{(i)}q^\nu\right), \quad (16)$$

thus ignoring a possible dependence of the form factors on the off-shell mass of the intermediate proton. The on-shell form factors are given by

$$F_j^{(i)}(q^2)=F_j^S(q^2)+F_j^V(q^2)\tau_3^{(i)}=F_j^S(q)+F_j^V(q). \quad (17)$$

For proton-proton bremsstrahlung with real photons $q^2=0$, and the NNγ vertex reduces to

$$\Gamma_\mu^{(i)}(q)=e\left(\gamma_\mu^{(i)}-\frac{i\kappa}{2M}\sigma_{\mu\nu}^{(i)}q^\nu\right), \quad (18)$$

where e is the charge and κ is the anomalous magnetic moment of the proton, and we have used that all intermediate nucleons are proton, hence τ_3 always gives $+1$ when sandwiched between isospin states. With this choice of the vertex, the nuclear current as defined in Eq. (15) is conserved in the Bethe-Salpeter formalism, provided that the kernel is local $[V(k,p)=V(k-p)]$. Details of the proof are given in Appendix B.

Due to the presence of the photon in the final state, in general the NN T matrix is needed in different Lorentz frames. Usually the NN interaction is determined in the center-of-mass (c.m.) system of the nucleon pair. If we choose the c.m. system of the initial protons to calculate the amplitude, the T matrix for the diagrams involving the NN interaction after emission of the photon is obtained through the Lorentz structure of the T matrix

$$T(p',p;P)=\Lambda(\mathcal{L})T^{\mathrm{cm}}(\mathcal{L}^{-1}p',\mathcal{L}^{-1}p;\mathcal{L}^{-1}P)\Lambda^{-1}(\mathcal{L}). \quad (19)$$

Here $\Lambda=\Lambda^{(1)}\Lambda^{(2)}$ is the spinor transformation for the boost $\mathcal{L}$ from the calculation frame to the c.m. frame of the NN interaction. Choosing the z direction to be defined by the photon momentum, the boost is given by

$$\mathcal{L}_\mu^\nu=\begin{bmatrix}\sqrt{1+\eta} & 0 & 0 & -\sqrt{\eta}\\ 0 & 1 & 0 & 0\\ 0 & 0 & 1 & 0\\ -\sqrt{\eta} & 0 & 0 & \sqrt{1+\eta}\end{bmatrix}, \quad (20)$$

where $\sqrt{\eta}=q/M_{\mathrm{pp}}$ and $\sqrt{1+\eta}=(2E-q)/M_{\mathrm{pp}}$. E is the total energy of the initial protons in their c.m. frame and we have defined an effective "proton-proton mass" $M_{\mathrm{pp}}=2\sqrt{E(E-q)}$. The corresponding one-particle spinor transformation operator is

$$\Lambda(\mathcal{L})=\sqrt{\frac{2E-q+M_{\mathrm{pp}}}{2M_{\mathrm{pp}}}}\left[\mathbf{1}-\gamma^0\gamma^3\frac{q}{2E-q+M_{\mathrm{pp}}}\right] \quad (21)$$

with $\mathbf{1}$ the identity matrix. In all calculations presented below the boosts are taken into account.

For the rescattering contribution an integration over the four-momentum k has to be performed. Again we would like to make a quasipotential reduction to simplify the integration. Such a reduction must be consistent with the approximation made in solving the T matrix. We have used the equal-time framework, where it is assumed that the NN interaction does not depend on the relative energy of the two nucleons in its center-of-mass system. Then the integration over the relative energy k_0 can be done analytically, since the integrand is of the form

$$I_0^{(i)}=\int\frac{dk_0}{2\pi}S^{(i)}(k_0,\mathbf{k}-\mathbf{q};E')\Gamma_\mu^{(i)}(q)S_2(k_0,\mathbf{k};E), \quad (22)$$

where $E'=E-\omega$ with ω the energy of the photon. A contour integration over k_0 can be carried out, resulting in three terms, which are given by the residues at the poles where one of the intermediate nucleon is on-shell. The poles of the two-nucleon propagator $S_2(k,P)$ are at

$$k_0^a=E+E_k-i\varepsilon,\quad k_0^c=E-E_k+i\varepsilon,$$

$$k_0^b=-E+E_k-i\varepsilon,\quad k_0^d=-E-E_k+i\varepsilon, \quad (23)$$

and the poles of the one-particle propagator $S^{(1)}(k',P')$ are at

$$k_0^e=(\omega-E)+E_{\mathbf{k}-\mathbf{q}}-i\varepsilon,\quad k_0^f=(\omega-E)-E_{\mathbf{k}-\mathbf{q}}+i\varepsilon. \quad (24)$$

If we choose to close the contour in the upper half-plane, we get contributions from pole k_0^c, k_0^d, and k_0^f. The first of these corresponds to the spectator model, where particle 2 is on its mass shell. The remaining three-dimensional integration has to be done numerically. An analysis of the pole structure of the remaining integrand shows that there are two poles in the spatial momentum $\mathbf{k}$, both arising from the spectator term. These poles correspond to the situation where either before or after emission of the photon the two protons are on-shell. In Appendix C a detailed discussion of these poles is given.

Physical observables

As mentioned the interesting dynamics of the bremsstrahlung process is contained in the amplitude M_{fi}, which is invariant under Lorentz boost. However, to compare to experiment physical observables have to be calculated, and since these are not necessarily invariant under Lorentz transformations, a particular reference frame has to be chosen. Measurements are done with a fixed target and a beam of definite energy T_{lab}. Thus the incoming proton defines a particular axis, which we take to be the z direction. There is still an arbitrariness in the definition of the xz plane, which we take to be defined by the direction of the photon. Then laboratory frame is defined such that the four momenta of the particles are

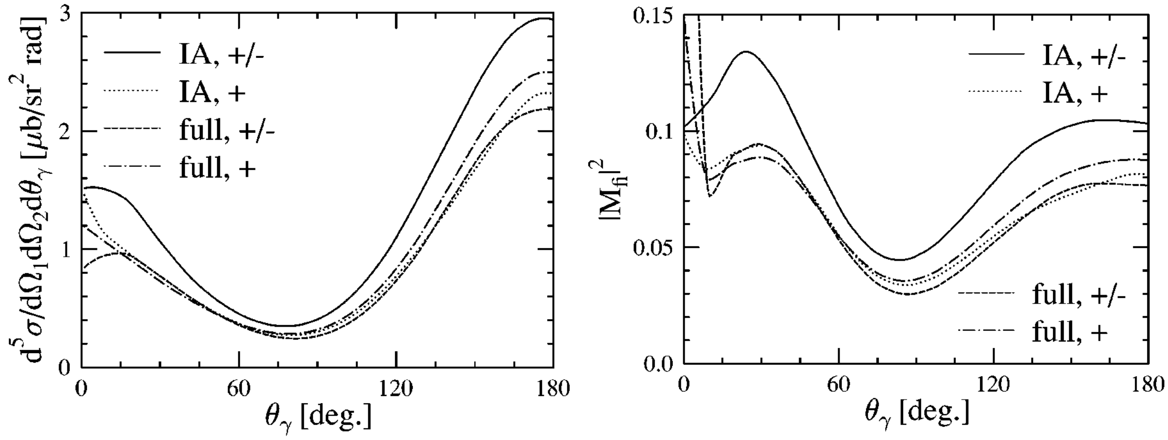

FIG. 2. The cross section and amplitude squared as a function of the photon angle θ_γ for $T_{\rm lab}=280$ MeV, $\theta_1=12°$, and $\theta_2=12.4°$. The IA shows a large difference between a calculation including negative-energy states (dashed line) and without (dashed-dotted line), of the order of 50%. If we include the rescattering contribution in the calculation, the difference between a calculation with (full line) and without (dotted line) negative-energy states is smaller, though still appreciable (~ 20). This is most readily seen in the figure where we show the invariant-amplitude squared.

$$p_1^\mu=(T_{\rm lab}+m,0,0,p_{\rm lab}),$$

$$p_2^\mu=(m,0,0,0),$$

$$p_1'^\mu=(E_1',p_1'\sin\theta_1\cos\phi_1,p_1'\sin\theta_1\sin\phi_1,p_1'\cos\theta_1),$$

$$p_2'^\mu=(E_2',p_2'\sin\theta_2\cos\phi_2,p_2'\sin\theta_2\sin\phi_2,p_2'\cos\theta_2),$$

$$q^\mu=(q,\sin\theta_\gamma,0,\cos\theta_\gamma). \tag{25}$$

In most experiments so far the energy of the incoming proton is fixed, and in this case there are only five independent variables due to energy and momentum conservation. Here we choose these to be the angles of the outgoing protons, $\theta_1,\phi_1,\theta_2,\phi_2$, and the angle of the photon, θ_γ.

With this choice of dependent and independent variables the cross section in the lab system is given by

$$\frac{d^5\sigma}{d\Omega_1 d\Omega_2 d\theta_\gamma}=\frac{m^3 p_1'^2 p_2'^2 q}{pE_1'E_2' 2\omega(2\pi)^5 N_a}\overline{\sum_{\lambda_i\lambda_f}}|M_{fi}|^2, \tag{26}$$

where

$$N_a=\frac{p_1'}{E_1'}(\sin\theta_2\cos\theta_\gamma\cos\phi_2-\cos\theta_2\sin\theta_\gamma)$$
$$+\frac{p_2'}{E_2'}(\sin\theta_\gamma\cos\theta_1-\cos\theta_\gamma\sin\theta_1\cos\phi_1)$$
$$+\frac{q}{\omega}(\sin\theta_1\cos\theta_2\cos\phi_1-\cos\theta_1\sin\theta_2\cos\phi_2), \tag{27}$$

and $\overline{\Sigma}$ implies averaging over initial spins λ_i and summing over final spins λ_f. For real bremsstrahlung $\omega=q$ and all factors q/ω are equal to 1 in Eqs. (26)–(28). The analyzing power is then defined as

$$A_y=\frac{d\sigma^\uparrow-d\sigma^\downarrow}{d\sigma^\uparrow+d\sigma^\downarrow} \tag{28}$$

with $d\sigma^\uparrow$ the differential cross section for incoming proton 1 with spin in the $+\hat{y}$ direction and $d\sigma^\downarrow$ the differential cross section for incoming proton 1 with spin the $-\hat{y}$ direction.

IV. RESULTS

The ppγ amplitude constructed with the T matrix that is found from the Bethe-Salpeter equation, or the BSLT approximation to that equation, contains negative-energy states in a dynamical way. Since the intermediate nucleon in the bremsstrahlung process is off-shell, these negative-energy states in principal should be included. As we have argued in a recent paper [15], the effects of including these intermediate states are of the same order of magnitude as contributions from the Δ and meson-exchange currents. Furthermore the energy transfer in the NN interaction is nonzero, giving rise to retardation effects.

We will first discuss the influence of negative-energy states using an equal-time approximation for the NN interaction, thus effectively ignoring the retardation effects. The lowest-order approximation is to include only the contributions from negative-energy states in the single-scattering diagram. We will show that for an accurate description of the bremsstrahlung amplitude it is essential also to include the contributions arising from the rescattering contributions. As a second point we will address the importance of the retardation effects in the NN interaction.

A. The contribution from negative-energy states

Both the single-scattering and rescattering diagrams contain contributions from negative-energy states. In a calculation including only positive-energy states the contributions from the rescattering diagram are of the order of 20%. Therefore it seems reasonable to expect that the impulse approximation gives the main contribution from negative-energy states. In the left panel of Fig. 2 we show the cross section for the bremsstrahlung process at incoming proton energy $T_{\rm lab}=280$ MeV and fixed outgoing proton angles $\theta_1=12°$, $\theta_2=12.4°$ as a function of photon angle θ_γ using only the

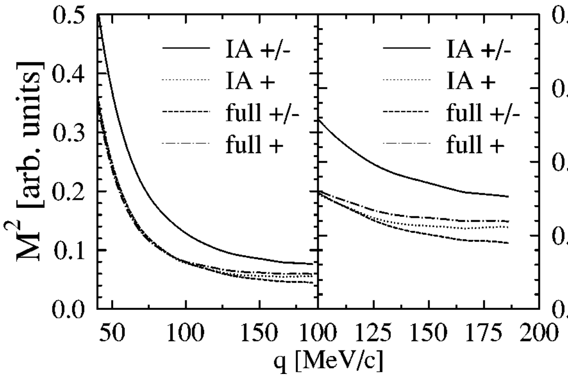

FIG. 3. The square of the ppγ amplitude as a function of the photon momentum q for fixed center-of-mass angles $\theta_1=36°$, $\theta_2=69°$ and $\theta_\gamma=124°$. The photon momentum was varied by varying the energy of the incoming proton, T_{lab}. Shown are the amplitudes including the rescattering contribution with (full line) and without (dotted line) negative-energy states coupling to the photon. Also shown are the amplitudes calculated with only the single-scattering contributions with (dashed line) and without (dashed-dotted line) negative-energy states coupling to the photon.

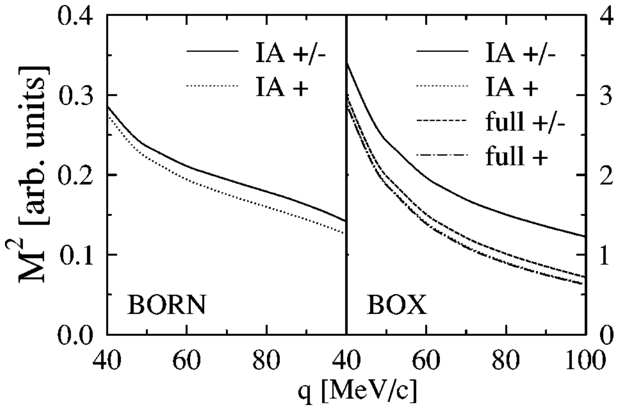

FIG. 4. Invariant-amplitude squared for fixed $E_{\mathrm{lab}}=140$ MeV and photon angle $\theta_\gamma=170°$. The left panel shows the Born result, the right panel shows a calculation with the box diagram. In the Born case there is no noticeable difference between a calculation including negative-energy state contributions (full line, IA $+/-$) and without (dotted line, IA $+$). In the case of the external box diagrams the difference between a calculation including negative-energy state contributions (full line, IA $+/-$) and without (dotted line, IA $+$) is large and in lowest order independent of q. Only if we include the internal diagrams (respectively dashed line, IA $+/-$ and dashed-dotted line, IA $+$) the negative-energy state contributions cancel.

single-scattering diagrams. The full line is a calculation including both positive- and negative-energy states, while the dashed line is the result if we include only positive-energy states. The intermediate negative-energy states give a large contribution over the entire range of photon angles, which is more clearly seen when plotting the square of the amplitude (i.e., the cross section without phase-space factor), as we have done in the right panel of Fig. 2. At this kinematics the cross section is dominated strongly by (uninteresting) phase-space characteristics.

If we include the rescattering contributions, the net influence of negative-energy states is reduced. This is also shown in Fig. 2, where the dashed line is a calculation including only intermediate positive-energy states, and the dashed-dotted line is the result for the full calculation, including also the contributions from negative-energy states. We see that there is a large cancellation between the contributions of negative-energy states from the single-scattering and the rescattering diagrams. The net result is that the contribution of negative-energy states is in general smaller, but overall an effect of the order of 20% remains. Confining ourself to the only positive-energy state contributions, it is interesting to note that the single-scattering contribution is close to the full calculation, except again at the extreme photon angles, where the (positive-energy) rescattering contributes significantly.

The negative-energy states are essentially of relativistic origin, and therefore one would expect that the effects depend strongly on the energies of the protons and the photon. To illustrate this dependence on the photon momentum q, in Fig. 3 we show the square of the amplitude as a function of the photon momentum for fixed proton angles and varying incoming proton energy T_{lab}. We compare a calculation in the IA with negative-energy states (the full line) and without negative-energy states (the dashed line), and a calculation including the rescattering contribution, again with (the dashed-dotted line) and without (the dotted line) negative-energy states. In the left panel we show the behavior over the photon momentum range from 10 MeV/c to 200 MeV/c, whereas the right panel is a blowup of the high momentum region. For the IA the negative-energy states give a considerable contribution over the whole momentum range, whereas for the full calculation the contributions from negative-energy states in the rescattering diagrams tend to cancel those from the single-scattering diagrams, effectively giving only a sizable contribution in the high momentum region.

As is well known, the dominant contributions to Compton scattering at low photon momenta are solely from the Z graphs [16]. In this connection the cancellation in the bremsstrahlung case between the contributions of negative-energy states from the rescattering diagram and those from the single-scattering diagrams at first seems rather puzzling, since the rescattering diagram does not contribute in the lowest order of the strong-coupling constant g^2. Hence a cancellation of Z graphs should already take place in this order in the single-scattering contributions. Let us replace the NN T matrix by the OBE kernel in the bremsstrahlung calculation. The calculated results for the single-scattering diagram in this approximation is shown in the left panel in Fig. 4, where the invariant-amplitude squared is plotted as a function of the photon momentum q. To obtain this dependence the proton angles $\theta_1=\theta_2$ have to be varied simultaneously. From this figure we see that in contrast to the Compton scattering case the negative-energy states here indeed lead to vanishing contribution at low photon momentum, while the effects are of the order of 20% at the higher photon momenta, similarly as found in the full calculation.

Considering the diagrams one order higher in the strong-coupling constant (the box diagrams) we may explicitly verify that the internal radiation diagram is essential to achieve cancellation of the large Z-graph contribution of the single-scattering diagram. This is shown in the right panel in Fig. 4: the sum of the diagrams where the photon couples to the external proton give a large contribution of negative-energy states, whereas the addition of the diagram where the photon couples to the internal proton kills most of the effect.

The observed cancellation is a consequence of the low-energy theorem for bremsstrahlung [17]. This theorem states that for low photon momenta (as compared to the internal excitation energy of the nucleon, the mass of the pion), the NN-bremsstrahlung amplitude can be expanded as

$$M_\mu=\frac{A}{q}+B+Cq+\mathcal{O}(q^2) \tag{29}$$

as is demonstrated in detail in Appendix D. The constants A and B only depend on the static properties of the nucleon, its charge and magnetic moment, and the on-shell NN interaction, whereas the constant C and the other higher-order terms can contain off-shell contributions.

Derivatives of the T matrix in the on-shell direction contribute to the constant B. The contributions from negative-energy states are contained in these derivatives. This is clearly seen in a description with only positive-energy states, where they are replaced by contact terms. As is the case in Compton scattering [18], these terms may contribute significantly in the low-energy limit. In order to see whether (and if so, how) the low-energy theorem for bremsstrahlung indeed implies that negative-energy states only contribute to the terms of order q and higher in the expansion in the photon momentum, we first consider the case of bremsstrahlung from a spin-$\frac{1}{2}$ particle with initial momentum $\frac{1}{2}P+p$ and final momentum $\frac{1}{2}P'+p'$ interacting through an interaction V with a second spin-$\frac{1}{2}$ particle with momenta $\frac{1}{2}P-p$ and $\frac{1}{2}P'-p'$. First consider the case that the second particle is uncharged. Conservation of total momentum gives $P'=P-\frac{1}{2}q$, whereas momentum conservation at the photon vertex gives $p'=p-\frac{1}{2}q$. The leading-order contribution in the expansion from intermediate negative-energy states due to the emission of the photon prior to the interaction V is

$$\begin{aligned}M^{\mathrm{i}}_\mu&=\overline{\psi}(p',P')V\left(p',p-\frac{1}{2}q;P-\frac{1}{2}q\right)\\&\quad\times\frac{\Lambda_-^{(1)}(\mathbf{p}+\mathbf{q})}{E_p+E_{\mathbf{p}+\mathbf{q}}}\gamma_\mu^{(1)}\psi(p,P)\\&=\overline{\psi}(p',P')V(p',p;P)\,\frac{-p_\mu+E_p\gamma_\mu^{(1)}\gamma_0}{2E_p^2}\psi(p,P)\\&\quad+\mathcal{O}(q),\end{aligned} \tag{30}$$

where $\psi(p,P)=u^{(1)}(\frac{1}{2}\mathbf{P}+\mathbf{p})u^{(2)}(\frac{1}{2}\mathbf{P}-\mathbf{p})$ and $\overline{\psi}(p',P')=\overline{u}^{(1)}(\frac{1}{2}\mathbf{P}'+\mathbf{p}')\overline{u}^{(2)}(\frac{1}{2}\mathbf{P}'-\mathbf{p}')$ are the initial and final states for the spin-$\frac{1}{2}$ particles, with u and $\overline{u}$ free Dirac spinors. Thus negative-energy states at lowest order contribute to the constant B, and since we are only interested in the model-independent terms the remaining q dependence in Eq. (30) has been ignored. We furthermore used that the projection operator acting on an on-shell spinor gives

$$\begin{aligned}\Lambda_-(\mathbf{p})\gamma_\mu u(p)&=\frac{E_p\gamma_0+\boldsymbol{\gamma}\cdot\mathbf{p}-M}{2E_p}\gamma_\mu u(p)\\&=\frac{2E_pg_{0\mu}-2p_ig_{i\mu}+\gamma_\mu(\not{p}-m-2E_p\gamma_0)}{2E_p}\\&\quad\times u(p)\\&=\frac{-p_\mu+E_p\gamma_0\gamma_\mu}{E_p}u(p),\end{aligned} \tag{31}$$

since $p_\mu=(E_p,-\mathbf{p})$. The emission from the photon after the interaction V gives rise to a similar term M^{f}_μ, and to first order the contributions from negative-energy states is $M_\mu=M^{\mathrm{i}}_\mu+M^{\mathrm{f}}_\mu$,

$$\begin{aligned}M_\mu&=\overline{\psi}(p',P')\left(V(p',p;P)\,\frac{-p_\mu+E_p\gamma_0^{(1)}\gamma_\mu^{(1)}}{2E_p^2}\right)\psi(p,P)+\overline{\psi}(p',P')\left(\frac{-p'_\mu+E'_p\gamma_\mu^{(1)}\gamma_0^{(1)}}{2E^2_{p'}}V(p',p;P)\right)\psi(p,P)+\mathcal{O}(q)\\&=\frac{1}{2E_p}\,\overline{\psi}(p',P')[V(p',p;P),\gamma_0^{(1)}\gamma_\mu^{(1)}]\psi(p,P)-\frac{p'_\mu+p_\mu}{E_p^2}\,\overline{\psi}(p',P')V(p',p;P)\psi(p,P)+\mathcal{O}(q),\end{aligned} \tag{32}$$

where $1/E_{p'}=1/E_p+\mathcal{O}(q)$ and the interchange of γ_μ and γ_0 can be done since the zeroth component of M_μ is zero, which is most easily seen from Eq. (31) with $p_0=E_p$. Thus it is clear that for a system of two nonidentical spin-$\frac{1}{2}$ particles the contributions from intermediate negative-energy states in general do not vanish. For example, in the case that the interaction V is given by a one-boson exchange with scalar, pseudovector, and vector particles, the first term in Eq. (32) vanishes for the scalar and pseudovector parts (the last of which reduces to a simple pseudoscalar in the lowest order in q), while for a vector interaction a finite contribution remains. The propagator of a vector meson with momentum k and mass m_V is

$$\Delta_{\mu\nu}=-g_{\mu\nu}+\frac{k_\mu k_\nu}{2m_V}\Delta(k), \tag{33}$$

with $\Delta(k)$ is the scalar part of the meson propagator. The term proportional to k_ν vanishes for on-shell states for particle 2, since this gives a term $\not p_{2f}-\not p_{2i}=M_2-M-2=0$, so what remains is of the form

$$\begin{aligned} M_\mu^V &= \overline{\psi(p',P')}[V^V,\gamma_0^{(1)}\gamma_\mu^{(1)}]\psi(p,P) \\ &= \overline{\psi(p',P')}[\gamma_\nu^{(1)}\Delta(k)\gamma^{(2),\nu},\gamma_0\gamma_\mu]\psi(p,P) \\ &= \overline{\psi(p',P')}(2g_{\nu 0}\gamma_\mu-2g_{\nu\mu}\gamma_0)^{(1)}\Delta(k)\gamma_\nu^{(2)}\psi(p,P) \\ &= \overline{\psi(p',P')}2(\gamma_\mu^{(1)}\gamma_0^{(2)}-\gamma_0^{(1)}\gamma_\mu^{(2)})\Delta(k)\psi(p,P). \end{aligned} \tag{34}$$

The situation is very similar to the case of Compton scattering [18,19]. There the vector particle is a real photon and the coupling to particle 2 as well as the propagator (33) are absent, and in fact the results obtained above can be used if the coupling to the second particle and the propagator of the vector particle are left out. Hence the contribution from negative energy states in Compton scattering is

$$\begin{aligned} M_{\mu\nu}^{\text{Compton}} = \overline{u(p')}\,\frac{1}{2E_p}\Bigg[& 2g_{\nu 0}\gamma_\mu-2g_{\nu\mu}\gamma_0 \\ & -\left(\frac{p'_\mu+p_\mu}{E_p}\right)\gamma_\nu\Bigg]u(p). \end{aligned} \tag{35}$$

The pole term in the low-energy expansion is absent and the first term in Eq. (35), corresponding to Eq. (34), gives the low-energy limit for forward Compton scattering (the Thomson limit).

For the case of two identical, charged, spin-$\frac{1}{2}$ particles the emission of the photon by particle 1 again gives Eq. (32). However, particle 2 gives rise to a similar contribution. Thus for the sum of contributions from both particles the second term in Eq. (32) vanishes in lowest order in q, which is most readily seen in the c.m. system where the spatial momenta of particles 1 and 2 are equal in size but opposite. Again for the first term the contributions from scalar and pseudovector mesons vanish, but furthermore the contribution from the vector meson is zero, since a similar term as in Eq. (33) arises from emission from particle 2, except that the first and second term are interchanged. Since they have opposite sign, the result is that for a one-boson exchange with scalar, pseudovector, and vector mesons the contribution from negative-energy states vanishes. Aside from the cancellation between emission from initial and final states of a charged particle, apparent from the commutator in Eq. (32), there is a cancellation between emission from particle 1 and particle 2, which is clearly a result of the Pauli symmetry of the two spin-$\frac{1}{2}$ particles.

So far we have focused on a one-boson interaction. The conclusion with respect to the nonvanishing contributions in the case of one charged particle also holds for a general interaction, since there is no additional constraint that would cause the contributions to vanish. For the case of two identical spin-$\frac{1}{2}$ particles the derivation of the low-energy theorem is given in Appendix D. If we write the NN interaction as a function of the Lorentz invariants $p_1'^2$, p_1^2 and a parameter ν which for emission from the initial proton 1 is defined as $\nu=(p_1-q)\cdot p_2+p_1'\cdot p_2'$ and similar for the emission from the other legs, the result is that the amplitude in the low-energy limit is given by

$$\begin{aligned} M_\mu = e\overline{\psi(p',\tilde{p}')}\Bigg[& \left(\gamma_\mu^{(1)}-\frac{i\kappa}{2M}\sigma_{\mu\nu}^{(1)}q^\nu\right)\frac{\not p'+\not q+M}{2p'\cdot q}T_0 \\ & -T_0\frac{\not p-\not q+M}{2p\cdot q}\left(\gamma_\mu-\frac{i\kappa}{2M}\sigma_{\mu\nu}q^\nu\right)+\vec{D}_\mu^{(1)}(p')T_0 \\ & +T_0\overleftarrow{D}_\mu^{(1)}(p)\Bigg]\psi(p,\tilde{p})+(1\leftrightarrow 2)+\mathcal{O}(q), \end{aligned} \tag{36}$$

where with the exchange of the indices of particles 1 and 2 also the momenta in the propagators and projection operators are replaced by those of particle 2, and we have defined a differential operator

$$D_\mu^{(i)}(p)=\frac{p_\mu}{p\cdot q}q^\nu\frac{\partial}{\partial p^\nu}-\frac{\partial}{\partial p^\mu}. \tag{37}$$

The basic ingredient in the calculation of the amplitude is the sum of all terms contributing to the pole term A in Eq. (29), the external diagrams where a photon is emitted by one of the initial- or final-state protons. In our case this is the sum of all single-scattering contributions. The resulting amplitude violates current conservation, and the term $\partial/\partial p_\mu$ has to be introduced in the differential operator to ensure that the current is conserved. As a result derivatives of the T matrix in the off-shell direction vanish. The added term effectively is a combination of the rescattering contribution and contact term, where the photon couples to the NN interaction directly. Since the relativistic calculation can be shown to conserve the current if negative-energy states are included (Appendix B) the only contribution in this case is the rescattering diagram.

For the differential operator as defined in Eq. (37) the contributions from negative-energy states to the amplitude cancel. This can be seen by writing the T matrix in Eq. (36) as a sum of positive- and negative-energy contributions

$$T(p',p,\nu)=\gamma_0\Lambda_+T^+ + \gamma_0\Lambda_-T^-. \tag{38}$$

The differential operator then either acts on the T matrix, which for the negative-energy states gives no contribution (since $\overline{u_+}\gamma_0\Lambda_-=0$), or on the projection operators. Consider the contribution where the proton is emitted from the final proton 1. The contribution that arose from expanding the off-shell T matrix around the on-shell point is proportional to

$$\begin{aligned} q^\nu\frac{\partial\gamma_0\Lambda_-}{\partial p'^\nu} &= \frac{1}{2}q^\nu\frac{\partial 1/E'}{\partial p'^\nu}\gamma_0E'\Lambda_- + \frac{1}{2E'}q^\nu\frac{\partial}{\partial p'^\nu} \\ &\quad\times[\not p'-m+(E'-p_0)\gamma_0]\gamma_0 \\ &= -\frac{\mathbf{q}\cdot\mathbf{p}}{2E'^2}\gamma_0\Lambda_- + \frac{1}{2E'}\left(\not q-\frac{q\cdot p}{E'}\gamma_0\right)\gamma_0, \end{aligned} \tag{39}$$

and the first term in this expression does not give a contribution, since the projection operator acts on the external spinor $\overline{u(p')}$, which gives zero. From Eq. (39) it follows immediately that the contribution added to enforce current conservation gives a similar expression, and the net contribution from the differential operator acting on the negative-energy state projection operator is

$$D_{\mu}(p')\gamma_0\Lambda_-(p')=\left(\frac{p'_{\mu}}{p'\cdot q}q^{\nu}\frac{\partial}{\partial p'^{\nu}}-\frac{\partial}{\partial p'^{\mu}}\right)\frac{\not{p}'-M}{2E'}\gamma_0$$
$$=\left(\frac{p'_{\mu}\not{q}}{p'\cdot q}-\gamma_{\mu}\right)\frac{\gamma_0}{2E'}. \tag{40}$$

The other contributions from intermediate negative-energy states arise from the term with $\not{q}$ in the propagator and are proportional to

$$\overline{u(p')}\gamma_{\mu}\frac{\not{q}}{2p'_{\mu}\cdot q}\gamma_0\Lambda_-(p')$$
$$=\gamma_{\mu}\frac{\not{q}(\not{p}'-M)}{4E'(p'_{\mu}\cdot q)}\gamma_0$$
$$=\overline{u(p')}\gamma_{\mu}\frac{[q^{\nu}p'^{\sigma}(-\gamma_{\sigma}\gamma_{\nu}+2g_{\nu\sigma})-M\not{q}]}{4E'(p'_{\mu}\cdot q)}\gamma_0$$
$$=\overline{u(p')}\left(-\frac{p'_{\mu}\not{q}}{p'\cdot q}+\gamma_{\mu}\right)\frac{\gamma_0}{2E'}, \tag{41}$$

where in the last line we have used that $\overline{u_+}(p)(\not{p}+M)=2p_{\mu}\overline{u_+}(p)$. Comparing the expressions in Eqs. (40) and (41) it is clear that the contributions from negative-energy states cancel in the low-energy limit.

The result that negative-energy contributions to the bremsstrahlung amplitude vanish for a general NN interaction is clearly due to the inclusion of the second term in the differential operator D_{μ}. It implies that the bremsstrahlung process can be described in terms of positive-energy states only, provided that additional counter terms are included such that current conservation is satisfied. Part of these terms are the rescattering contribution, while part of these are contact terms. The contact terms are an effective way of including the contributions from negative-energy states, and in principle contribute to the nonsingular term in the expansion of the amplitude [the constant B in Eq. (29)]. We again can compare to the case of Compton scattering, where in a calculation with only positive-energy states a photon-photon-nucleon term has to be included to find the correct low-energy limit.

In the case of proton-proton bremsstrahlung the current calculated from the single-scattering and rescattering diagrams is conserved when both positive- and negative-energy states are included. Thus the addition of the second term in the differential operator D_{μ} corresponds to the inclusion of the rescattering contribution in a full calculation, and no contact terms are necessary. Furthermore, we have seen that for the OBE interaction the negative-energy states do not contribute, and therefore the contact terms corresponding to negative-energy states in a calculation including only positive-energy states, which are in general necessary to satisfy current conservation, are zero for this particular process. Hence for proton-proton bremsstrahlung negative-energy states do not contribute in the low-energy limit.

If we compare our results with other calculations we see that the calculations including only positive-energy states are

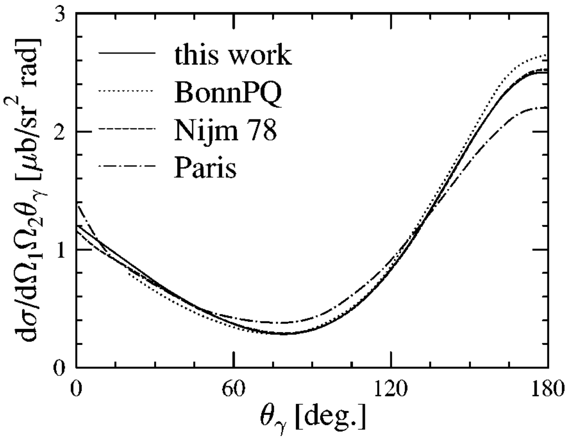

FIG. 5. The cross section calculated with the T matrix with only positive-energy states, but retaining the small components of the nucleon spinor, as compared to calculations using a potential model, including relativistic spin corrections. The differences between the T-matrix calculation and the nonrelativistic calculations are of the same order as those between the nonrelativistic calculations themselves.

in agreement with nonrelativistic potential-model calculations that include relativistic spin corrections. The comparison should be done with this type of calculation, since we use the full four-component spinor, and the small components are kept. In Fig. 5 we illustrate this by comparing our results with the Bonn PQ T matrix calculation [20] and a calculation using the Nijmegen potential at $T_{\mathrm{lab}}=280$ MeV, $\theta_1=12°$, $\theta_2=12.4°$. The full line is our result when including only positive energy in the single-scattering and rescattering contributions, and the result differs only little from the calculations using the Bonn (the dotted line) or Nijmegen (the dashed line) interactions. For this particular kinematics we see some deviations, in particular at forward and backward photon angles. These differences are due to a somewhat different on-shell behavior of the t matrices.

The large contribution from the negative-energy states in the impulse approximation has also been reported by de Jong and Nakayama [3], who used a T matrix generated from the Gross equation [4]. However, if we compare the results including rescattering contributions, we see in particular for the cross section that the contributions of negative-energy states is substantially enhanced in our calculation. On the other hand, for the analyzing power the effects of negative-energy states are rather similar. The main difference in the two calculations is the type of quasipotential reduction that is used. Assuming that retardation effects in the positive- and negative-energy states behave similar, we can approximate their calculation by including only the spectator contribution to the rescattering diagram. The result is that for the cross section the net contribution from negative-energy states is reduced whereas for the analyzing power the contribution is somewhat enhanced, thus giving a result that is similar to that reported by de Jong and Nakayama. Concluding we can say that the contributions from the nonspectator terms are essential to give a full description at higher momenta. The suppression of the cross section due to the inclusion of intermediate negative-energy states is of the same order of magnitude as the effects reported by Eden and Gari [21], although they find considerably higher values for the absolute

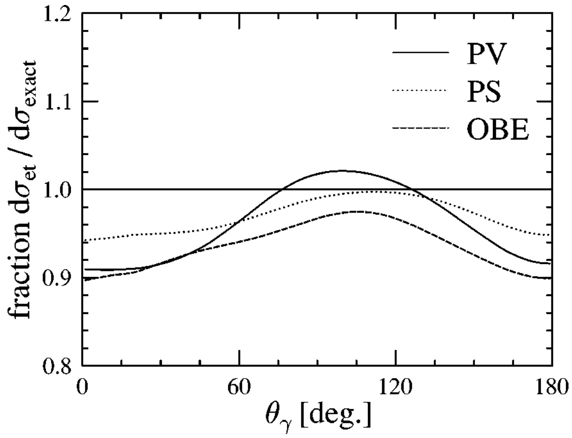

FIG. 6. The effect of the equal-time approximation in the bremsstrahlung process at $T_{\text{lab}}=280$ MeV, $\theta_1=12°$ and $\theta_2=12.4°$. Shown is the fraction of the cross section calculated using the equal-time approximation to a full calculation, for the one-pion exchange with a pseudoscalar coupling (full line) and a pseudovector coupling (dotted line) and the OBE kernel (dashed line). From case of the pseudoscalar NNπ coupling it is clear that retardation effects in the meson propagator are small.

value of the cross section. This may be primarily due to the positive-energy contribution, for which case their prediction differs substantially from ours and the nonrelativistic model calculations.

B. Retardation effects in the NN interaction

In the calculation of the bremsstrahlung amplitude we use the equal-time or instantaneous framework. In this framework it is assumed that the t matrices can be evaluated at the point where the relative energy of the protons k_0 is zero in the center-of-mass system of the interaction. To investigate the effects of retardation in the NN interaction we may first look at a simple one-pion exchange (OPE) model without form factors, where the NNπ vertex was either assumed to be given by a pseudovector ($\not k\gamma_5$) or pseudoscalar (γ_5) coupling. The nuclear current for emission from particle i in the equal-time approximation is given by

$$J_\mu^{(i)}=\widetilde{V}^{\text{OPE}}(k'^{\text{cm}})S^{(i)}(p'+\tfrac{1}{2}q,P')\Gamma_\mu^{(i)}(q)|_{k_0'^{\text{cm}}=0} + \Gamma_\mu^{(i)}(q)S^{(i)}(p-q,P)\widetilde{V}^{\text{OPE}}(k^{\text{cm}})|_{k_0^{\text{cm}}=0}, \tag{42}$$

where $\widetilde{V}$ is the one-pion exchange boosted from the center-of-mass system of the interaction to the lab frame and k^{cm} and k'^{cm} are the four momenta of the pion in the c.m. frame. In Fig. 6 we show the cross section calculated with the equal-time approximation divided by the result of the calculation using the exact one-pion exchange, just below the pion production threshold, $T_{\text{lab}}=280$ MeV, and small proton angles $\theta_1=12°$, $\theta_2=12.4°$. For the pseudoscalar coupling the result is close to 1 at all photon angles, so that we can conclude that retardation effects in the meson propagator are small. For the pseudovector coupling we see larger deviations, up to 15%, so that it is clear that retardation effects in the nucleon-nucleon meson coupling can be considerable. If we use the one-boson exchange kernel instead of the OPE interaction, the effects are of the same order as those found for the pseudovector coupling, as can also be seen in Fig. 6, where the dashed line is the fraction of the cross section calculated with the OBE kernel in the equal-time approximation to the cross section calculated with the exact OBE kernel. The effects are mainly due to the pion and the vector ω meson.

To see whether these retardation effects also can be substantial in the T matrix calculations, we have constructed a modified equal-time approximation by iterating one full one-boson exchange,

$$T^{\text{met}}(p',p;P)=V^{\text{OBE}}(p',p)-i\int\frac{d^4k}{(2\pi)^4}V^{\text{OBE}}(p',\hat{k}) \times S_2^{\text{BSLT}}(\hat{k},P)T^{\text{et}}(\hat{k},p;P), \tag{43}$$

in the c.m. system of the incoming nucleon pair, where the relative energy of the incoming nucleons $p_0=0$, and $\hat{k}$ is restricted through the BSLT approximation. T^{met} is the modified equal-time T matrix, whereas T^{et} is the T matrix calculated with the equal-time approximation. Note that the two T matrices are on-shell equivalent. The relative energy of the final nucleon pair is calculated by assuming that particle 2 is on-shell, so that $p_0'=E_{p'}-E_p$. In Fig. 7 we show a calculation of the cross section (left panel) and square of the amplitude (right panel) in the impulse approximation at the same kinematics as in the OPE calculation. The full line is the result using the modified equal-time T matrix, the dotted line is the result when we use T^{et}. The retardation effects are somewhat lower than in the case of the OPE, but as these energies and angles still appreciable, of the order of 10%.

In the construction of the k_0 dependence it is assumed that only one of the particles is on the mass shell. Furthermore the full k_0 dependence in the meson propagator is retained. Since this dependence will give rise to spurious poles [4], this formalism cannot be applied without modification to the rescattering contribution. However, the main interest is the effect of retardation in the meson propagator, which may be expected to cancel out in the integration over the three momentum in the rescattering loop. Furthermore we have seen that the effect is at most on the order of 10%, and thus the calculation restricting the use on the modified equal-time approximation to the impulse approximation may be assumed to give a reasonable estimate of the size of these effects.

C. Boost effects

In all calculations presented in the previous sections the boost from the center-of-mass system of the NN interaction to the calculation frame were taken into account. This was done by boosting the NN interaction through the transformation (20). The effects of this boost are of order q/M, and become sizable at higher energies. For example, at the kinematics of the TRIUMF experiment chosen to maximize the off-shell effects ($T_{\text{lab}}=280$ MeV, $\theta_1=12°$, $\theta_2=12.4°$) the boost effects are of the order of 5%. This is in agreement with the effects reported by Eden and Gari [2].

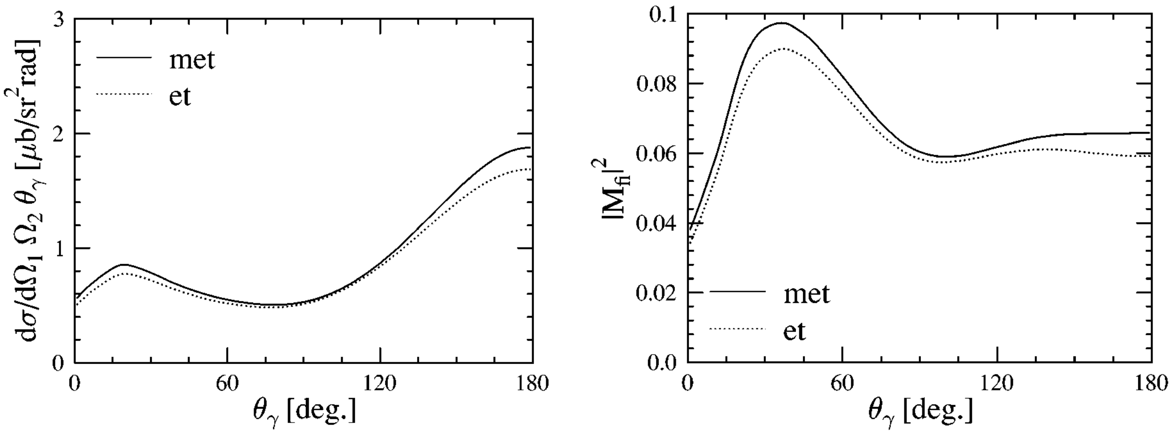

FIG. 7. The result for the modified equal-time approximation compared for a calculation in the impulse approximation just below the pion-production threshold, $T_{\rm lab}=280$ MeV, $\theta_1=12°$, $\theta_2=12.4°$ as a function of the photon angle θ_γ. The left (right) panel shows the cross section (amplitude squared). The full line is the result using the modified equal-time T matrix and the dotted line is the result using the equal-time approximation. Retardation effects are at most 15% for forward and backward photon angles, but generally of the order of 10%.

V. COMPARISON TO EXPERIMENT

Using the relativistic NN force, we have calculated bremsstrahlung for the TRIUMF [5] kinematics. In Fig. 8 our predictions are shown together with the experimental data. The upper plots show the cross section at proton angles $\theta_1=12°$, $\theta_2=12.4°$ (left) and $\theta_1=28°$, $\theta_2=12.4°$ (right) for the cross section, while the lower plots are the results for the analyzing power at $\theta_1=14°$, $\theta_2=12.4°$ (left) and $\theta_1=28°$, $\theta_2=12.4°$ (right). The theoretical predictions for the complete calculation including both positive- and negative-energy states are given by the solid lines, while the dotted line is a calculation including only positive-energy states. All calculations include boost effects. Retardation effects in the NN interaction are ignored. As discussed above, including these may increase the calculated cross section by about 10% for forward and backward angles. The data do not include the normalization factor 2/3.

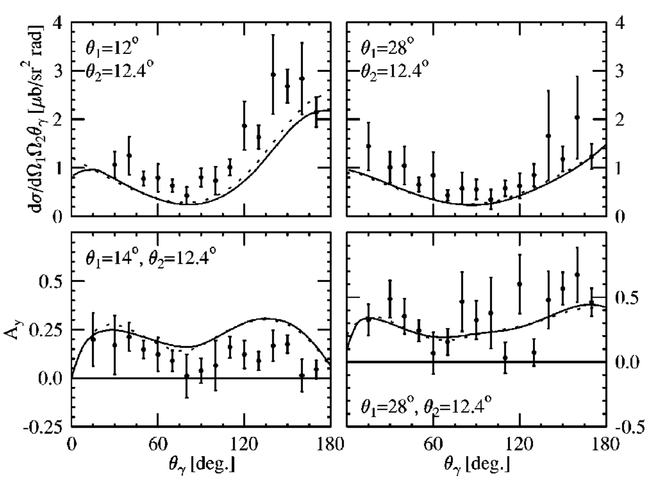

FIG. 8. Comparison of the calculated cross section (top) and analyzing power (bottom) to the experimental data from the TRIUMF experiment (with $E_{\rm lab}=280$ MeV). Two different kinematical situations are shown, left: $\theta_1=12°(14°)$, $\theta_2=12.4°$, right: $\theta_1=28°$, $\theta_2=12.4°$. The full line is a calculation including negative-energy states, the dotted line is with only intermediate positive-energy states.

The inclusion of negative-energy states tends to reduce the cross section for this kinematics. Since the calculation with only positive-energy states is in accordance with previous nonrelativistic calculations, the discrepancy between the theoretical predictions and the data remains and is even somewhat enhanced. Estimates [22,23] have been given for the contributions from meson-exchange currents. These were found to be small in the kinematical regions under consideration. Thus including these contributions would not explain the difference between theory and the TRIUMF experiment.

In Fig. 9 we show the predictions for, respectively, the cross section and the analyzing power at $T_{\rm lab}=500$ MeV as a function of the photon angle, with $\theta_1=\theta_2=10°$. The solid (dotted) curve is the result for the full calculation with (without) negative-energy states included, while the dashed (dashed-dotted) curve is the result for the IA calculation with (without) negative-energy states. Note that for the impulse approximation the inclusion of negative-energy states enhances the predicted cross section by a factor of 2 as compared to the result without negative-energy states, hugely overestimating the net effect of negative-energy states. Furthermore, for the full calculation the effects are of the order of 25–30 %, but extend over a larger region of phase space, and in general are more pronounced than the effects found at $T_{\rm lab}=280$ MeV. Similar large effects are seen in the analyzing power. On the basis of the low-energy theorem one would expect the effects of negative-energy states to be linear in the photon momentum as compared to the leading-order positive-energy state contribution. This is clearly not the case, since the photon energy at $T_{\rm lab}=500$ MeV is approximately twice as large as at 280 MeV. However, from the fact that negative-energy states contribute significantly already at $T_{\rm lab}=280$ MeV we can conclude that at these energies the low-energy theorem no longer is valid and the expansion of the invariant matrix elements breaks down.

In Fig. 10 we show the predictions for the cross section and analyzing power for the KVI [6] kinematics, with $T_{\rm lab}=190$ MeV incoming proton energy. A comparison is made with the soft-photon calculations of Ref. [7]. If we compare our calculation with only positive-energy states included (the dotted line) to the low-energy calculation (the dashed line), we see that at low proton angles, where the photon momentum is large, the predictions differ substan-

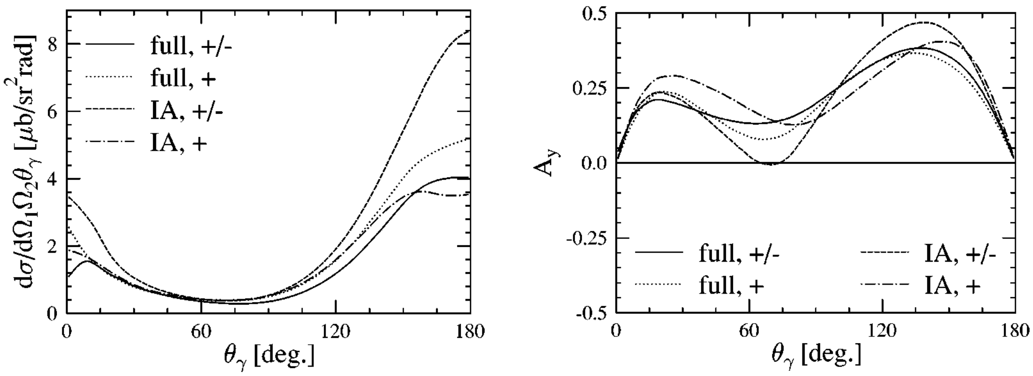

FIG. 9. The cross section (left) and analyzing power (right) at $T_{\mathrm{lab}}=500$ MeV with $\theta_1=\theta_2=10°$ as a function of the photon angle. The solid line is the full calculation, the dotted line is a calculation with only positive-energy states, whereas the dashed-dotted and dashed lines are the result using the IA, respectively, with and without negative-energy states included. For the cross section the effects of negative-energy states are of the order of 25–30 % in the full calculations. The effects in the analyzing power are clearly larger than for the calculation at $T_{\mathrm{lab}}=280$ MeV. The photon momentum is of the order of 125–200 MeV/c.

tially. This indicates that the higher-order terms in the expansion of the matrix elements give a significant contribution. At larger proton angles the predictions converge as expected, since there the photon momentum is smaller. The differences are even more clear in the analyzing power, a feature already noted in the discussion of the theoretical predictions for the TRIUMF experiment. Since the higher-order terms in the low-energy expansion are important, we have calculated the effects of negative-energy state contributions at this energy. The solid line gives the result of this calculation, and if we compare to the calculation including only positive-energy states (the dotted curve), we see that the effects of negative-energy states on both the cross section and the analyzing power is very small, except for small proton angles. However, the accuracy of the KVI experiment may be such that the effects predicted at smallest proton angles ($\theta_1=\theta_2=8°$) are significant.

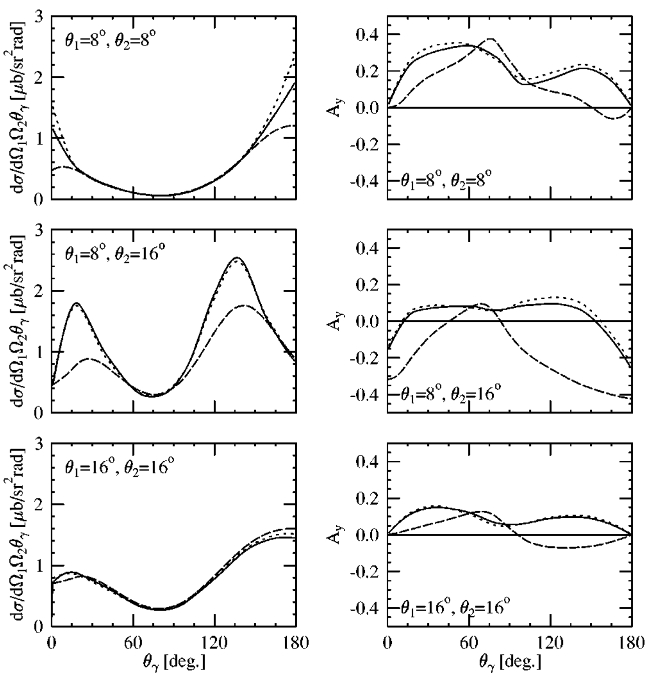

FIG. 10. The cross sections (left) and analyzing powers (right) at the kinematics of the KVI experiment, where $E_{\mathrm{lab}}=190$ MeV) at various proton angles as a function of the photon angle θ_γ. The full line is the calculation including negative-energy states, the dotted line has only intermediate positive-energy states, the dashed line is the soft-photon approximation calculation of Ref. [7].

It should be noted that although the relativistic OBE interaction parameters used in our study have not been obtained through a χ^2 fit [8,9,13] to the NN data, the resulting phase shifts are in reasonable agreement with experiment. In this connection we expect that a more refined relativistic interaction might change the absolute predictions somewhat, but that qualitatively the conclusions about the changes due to negative-energy states and retardation effects as studied in this paper will remain the same. An indication of the influence of modifying T may be obtained using the parameters from fit C [8]. The results differ by at most 10% in the kinematical situation under consideration for the calculation where only positive-energy states coupling to the photon were taken into account. The relative magnitude of the effects of negative-energy states remains unchanged.

VI. CONCLUSIONS

We have presented the results of a study of the effects of negative-energy states in the proton-proton bremsstrahlung process. The effects on the level of the impulse approximation are found to be appreciable. The rescattering contribution tends to cancel much of the effect which can be understood on the basis of the low-energy theorem for proton-proton bremsstrahlung. This is in contrast with the case of Compton scattering where the Z graphs play an essential role. The cancellation of the effects of negative-energy states was shown to result from the antisymmetry of the proton-proton initial and final state. Nevertheless, at higher photon momenta effects of the order of 20% were found from these Z-graph contributions. This leads to noticeable effects only at very particular kinematics for $T_{\mathrm{lab}}=190$ MeV, whereas for 500 MeV the effects show up clearly in the entire kinematical regime.

We furthermore investigated the retardation effects in the NN interaction by means of a simple one-pion exchange model, and found that these can be appreciable. A T matrix was constructed to incorporate some of these effects in the single-scattering contribution. Effects on the observables were found to be of the order of 10%. It would be interesting to also estimate these retardation effects in the rescattering diagram. Since the corrections are rather limited in size, this may be done by carrying out a lowest-order expansion of the NN T matrix in the relative energy variable.

We have also made a study of the limits of validity of the soft-photon approximation by Liou *et al.*, which should work well at low photon energies. We find in particular that at photon energies of the order of 100 MeV that there is a significant breakdown of that approximation. Comparing the predictions of the considered model with existing experimental data, we find that the discrepancies between the nonrelativistic theoretical predictions and the TRIUMF experiment cannot be attributed to the relativistic corrections. This is in accordance with other theoretical estimates. Clearly new and more accurate experiments are called for to settle this issue.

ACKNOWLEDGMENTS

This work is part of the research program of the ''Stichting voor Fundamenteel Onderzoek der Materie'' (FOM) with financial support from the ''Nederlandse Organisatie voor Wetenschappelijk Onderzoek'' (NWO).

APPENDIX A: DEFINITION OF SPINORS

The spinors used throughout the article are chosen according to the convention of Kubis [24]

$$u_\lambda^+(\mathbf{p})=N(p)\begin{bmatrix}1\\ \dfrac{2\lambda p}{E_p+M}\end{bmatrix}\xi_\lambda(\theta,\phi),$$

$$u_\lambda^-(\mathbf{p})=N(p)\begin{bmatrix}\dfrac{-2\lambda}{E_p+M}\\ 1\end{bmatrix}\xi_\lambda(\theta,\phi), \tag{A1}$$

where $N(p)=\sqrt{(E_p+M)/2E_p}$. These spinors satisfy the following normalization condition:

$$u_\lambda^{\rho\dagger}(\mathbf{p})u_{\lambda'}^{(\rho')}(\mathbf{p})=\delta_{\rho\rho'}\delta_{\lambda\lambda'}, \tag{A2}$$

which differs from the Bjorken and Drell [25] normalization constraint in the sense that usually $\overline{u}$ is chosen orthogonal to u. A consequence of this particular choice is that we now have

$$\sum_{\lambda,\rho} u_\lambda^\rho(\mathbf{p})\overline{u_\lambda^\rho}(\mathbf{p})=\gamma^0 \tag{A3}$$

instead of the identity. Thus whenever we substitute a full set of states for the identity, an additional γ^0 has to be included.

Using these spinors we can define operators $\Lambda_\rho \equiv\Sigma_\lambda u_\lambda^{(\rho)}(\mathbf{p})\overline{u_\lambda^{(\rho)}}(\mathbf{p})$,

$$\Lambda_+=\frac{E_p+M}{2E_p}\begin{bmatrix}\mathcal{I}_2 & \dfrac{-\mathbf{p}\cdot\boldsymbol{\sigma}}{E_p+M}\\ \dfrac{\mathbf{p}\cdot\boldsymbol{\sigma}}{E_p+M} & -\dfrac{\mathbf{p}^2}{(E_p+M)^2}\mathcal{I}_2\end{bmatrix}$$
$$=\frac{E_p\gamma_0-\mathbf{p}\cdot\boldsymbol{\gamma}+M}{2E_p},$$

$$\Lambda_-=\frac{E_p+M}{2E_p}\begin{bmatrix}\dfrac{\mathbf{p}^2}{(E_p+m)^2}\mathcal{I}_2 & \dfrac{\mathbf{p}\cdot\boldsymbol{\sigma}}{E_p+M}\\ \dfrac{-\mathbf{p}\cdot\boldsymbol{\sigma}}{E_p+M} & -\mathcal{I}_2\end{bmatrix}$$
$$=\frac{E_p\gamma_0+\mathbf{p}\cdot\boldsymbol{\gamma}-M}{2E_p}, \tag{A4}$$

from which Eq. (A3) follows. Due to the normalization condition the operators $\Lambda_\pm$ are not projection operators on the states $u_\pm$ (or $\overline{u_\pm}$). From the normalization it is clear that the true projection operator is $\gamma_0\Lambda^+\gamma_0$. However, the single nucleon propagator can be written in terms of the operators Λ, since from Eq. (A4) it follows that

$$\not{p}+M=(p_0+E_p)\Lambda_+(\mathbf{p})+(p_0-E_p)\Lambda_-(\mathbf{p}), \tag{A5}$$

and therefore

$$S(p)=\frac{\Lambda_+(\mathbf{p})}{p_0-E_p+i\epsilon}+\frac{\Lambda_-(\mathbf{p})}{p_0+E_p-i\epsilon}. \tag{A6}$$

APPENDIX B: CURRENT CONSERVATION

In this appendix we will prove that the nuclear current as defined in Eq. (15) is conserved. For ease of notation we introduce the continuum two-nucleon scattering state,

$$\Psi(k,p;P)=[(2\pi)^4\delta^4(p-k)-iS_2(k,P)T(k,p;P)]|p,P\rangle. \tag{B1}$$

The free nucleon pair $|p,P\rangle$ with relative momentum p and total momentum P is given by the antisymmetric combination of two free Dirac spinors. From this scattering state an ''amputated'' scattering state can be defined,

$$\phi(k,p;P)=[S_2^{-1}(k,P)(2\pi)^4\delta^4(p-k)-iT(k,p;P)]|p,P\rangle. \tag{B2}$$

Substitution of this amputated scattering state in the Bethe-Salpeter equation gives

$$T(p,p';P)|p',P\rangle = i[\phi(p,p',P) - S_2^{-1}(p,P)(2\pi)^4\delta^4(p'-p)|p',P\rangle]$$
$$= V(p,p')|p',P\rangle - i\frac{i}{(2\pi)^4}\int d^4k V(p,k)S_2(k,P)[\phi(p,p',P) - S_2^{-1}(k,P)(2\pi)^4\delta^4(p'-p)]|p',P\rangle$$
$$= \int \frac{d^4k}{(2\pi)^4} V(p,k)S_2(k,P)\psi(k,p';P). \tag{B3}$$

The initial and final states are on the mass shell, and consequently in the first line in Eq. (B3) the second term can be eliminated using $S_2^{-1}(p',P)|p',P\rangle = 0$. Thus the scattering state satisfies a homogeneous Bethe-Salpeter equation,

$$\phi(p,p';P) = \frac{-i}{(2\pi)^4}\int d^4k V(p,k)S_2(k,P)\phi(k,p;P). \tag{B4}$$

The e.m. current operator is assumed to be given by

$$\Gamma_\mu^{(i)}(q) = e\left[F_1^{(i)}(q^2)\gamma_\mu - \frac{i}{2M}F_2^{(i)}(q^2)\sigma_{\mu\nu}q^\nu\right] \tag{B5}$$

with e.m. nucleon form factors

$$F_n^{(i)}(q^2) = F_n^S(q^2) + F_n^V(q^2)\tau_3^{(i)}. \tag{B6}$$

In our particular case the photon is real, $q^2=0$, and the q dependence disappears from Eq. (B6). The current for emission from particle i then is found from substituting the scattering state (B2) in Eq. (15), which gives

$$J_\mu^{(i)} = \int \frac{d^4k}{(2\pi)^4}\overline{\phi(p',k';P')}S^{(i)}(k',P')\Gamma^{(i)}(q)S_2(k,P) \times\phi(k,p;P), \tag{B7}$$

where $P' = P - \frac{1}{2}q$, $k' = k - \frac{1}{2}q$ for emission from particle 1 and $k' = k + \frac{1}{2}q$ for emission from particle 2. The contribution with emission of the photon without strong interaction is absent, since the term that would arise from the sandwiching of the photon vertex with the in- and outgoing states vanishes, and Eqs. (B7) and (15) are indeed equivalent. The Ward identity for the photon vertex is

$$q\cdot\Gamma^{(i)}(q) = eF_1^{(i)}[S^{(i)^{-1}}(k',P') - S^{(i)^{-1}}(k,P)]. \tag{B8}$$

In the following we will concentrate on the contributions due to emission from particle 1; the derivation for emission from particle 2 is identical, except for this relative sign. The contraction of the nuclear current with the photon momentum is given by

$$q\cdot J^{(1)} = -ie\int \frac{d^4k}{(2\pi)^4}\overline{\phi(p',k',P)}S^{(1)}(k',P')F_1^{(1)} \times[S^{(1)^{-1}}(k',P') - S^{(1)^{-1}}(k,P)]S_2(k,P)\phi(k,p;P). \tag{B9}$$

The homogeneous BS equation (B4) can be substituted for $\overline{\phi}$ in the first term of the previous equation

$$\int \frac{d^4k}{(2\pi)^4}\overline{\phi(p',k')}S_2(k,P)\phi(k,p;P) = \int \frac{d^4k}{(2\pi)^4}\int\frac{d^4l}{(2\pi)^4}\overline{\phi(p',l;P')}S_2(l,P')V(l,k') \times S_2(k,P)\phi(k,p;P), \tag{B10}$$

whereas substitution for ϕ in the second term gives

$$\int \frac{d^4k}{(2\pi)^4}\overline{\phi(p',k';P)}S_2(k',P')\Psi(k,p) = \int \frac{d^4k}{(2\pi)^4}\int\frac{d^4l}{(2\pi)^4}\overline{\phi(p',k';P)}S_2(k',P')V(k,l) \times\phi(l,p;P). \tag{B11}$$

Applying the transformation $k\to k+\frac{1}{2}q$ in the second term and renaming l to k' in the first term and l to k in the second term, the result can be written as

$$q\cdot J^{(1)} = \frac{-ie}{(2\pi)^8}\int d^4k\int d^4k'\overline{\phi(p',k';P')}S_2(k',P') \times\left[V\left(k',k-\frac{q}{2}\right)F_1^{(1)} - F_1^{(1)}V\left(k'+\frac{q}{2},k\right)\right] \times S_2(k,P)\phi(k,p;P). \tag{B12}$$

In general the commutator of V and F does not vanish, even if the interaction V is local, $V(p,k)=V(p-k)$, due to a possible isospin dependence. In that case an extra contribution has to be included which is proportional to the commentator of V with $F^V\tau_3$. For the present NN interaction with the one-boson kernel that contains the isovector mesons π, ρ, and δ with isospin structure $\boldsymbol{\tau}^{(1)}\cdot\boldsymbol{\tau}^{(2)}$, the additional contribution is proportional to

$$[\boldsymbol{\tau}^{(1)}\cdot\boldsymbol{\tau}^{(2)},\tau^{(1)}]_3 = 2i(\boldsymbol{\tau}^{(1)}\times\boldsymbol{\tau}^{(2)})_3,$$
$$[\boldsymbol{\tau}^{(1)}\cdot\boldsymbol{\tau}^{(2)},\tau^{(2)}]_3 = -2i(\boldsymbol{\tau}^{(1)}\times\boldsymbol{\tau}^{(2)})_3. \tag{B13}$$

If the final and initial states, as well as all intermediate states, consist purely of protons, the commutators vanish and thus the additional terms needed for current conservation are absent.

In this proof we have made use of the fact that in the expression for the current and in the Bethe-Salpeter equations the same propagator structure is used. In practical calculations the BSLT approximation was used for the T matrix, while in the integration over the relative energy k_0 in

Eq. (B7) the equal-time approximation was made. Thus the T matrices were assumed not to depend on the relative energy in the c.m. system of the protons. Ignoring boost effects this implies that in Eqs. (B10) and (B11) the propagators that arise from substituting the homogeneous BS equation are to be replaced by BSLT propagators, and instead of Eq. (B12) we get

$$\begin{aligned} q\cdot J^{(1)}=e\int\int \frac{d^3k'}{(2\pi)^3}\frac{d^4k}{(2\pi)^4}\,\overline{\phi}^{\mathrm{BSLT}}(p',k';P') \\ \times S_2^{\mathrm{BSLT}}(k',P')V^{\mathrm{BSLT}}\left(k'-k+\frac{1}{2}q\right)S_2(k,P) \\ \times\phi^{\mathrm{BSLT}}(k,p;P)-e\int\int\frac{d^4k'}{(2\pi)^4}\frac{d^3k}{(2\pi)^3} \\ \times\overline{\phi}^{\mathrm{BSLT}}(p',k';P')S_2(k',P') \\ \times V^{\mathrm{BSLT}}\left(k'-k+\frac{1}{2}q\right)S_2^{\mathrm{BSLT}}(k,P) \\ \times\phi^{\mathrm{BSLT}}(k,p;P), \end{aligned} \tag{B14}$$

where ϕ^{BSLT}, S^{BSLT}, and V^{BSLT} are the scattering state, two-particle propagator, and one-boson kernel with four momenta restricted according to the BSLT prescription that the relative energy is zero in the c.m. system of the nucleons.

In the equal-time approximation the integration over the relative energy remains. The only dependence on this variable is in the full propagator S_2, and writing the propagators in terms of the projection operators [cf. Eq. (A6)] the integration over the contour closed in the upper half-plane gives for the first term in Eq. (B14)

$$\begin{aligned} &\oint\frac{k_0}{i\pi}S_2(k,P) \\ &\quad=\oint\frac{k_0}{i\pi}\left(\frac{\Lambda_+^{(1)}(\mathbf{k})}{E+k_0-E_k+i\epsilon}+\frac{\Lambda_-^{(1)}(\mathbf{k})}{E+k_0+E_k-i\epsilon}\right) \\ &\quad\quad\times\left(\frac{\Lambda_+^{(2)}(\mathbf{k})}{E-k_0-E_k+i\epsilon}+\frac{\Lambda_-^{(2)}(\mathbf{k})}{E-k_0+E_k-i\epsilon}\right) \\ &\quad=\frac{\Lambda_+^{(1)}(\mathbf{k})\Lambda_+^{(2)}(\mathbf{k})}{E_k-E}+\frac{\Lambda_-^{(1)}(\mathbf{k})\Lambda_-^{(2)}(\mathbf{k})}{E_k+E}, \end{aligned} \tag{B15}$$

since contributions are picked up from the term with $\Lambda_+^{(2)}$ at $k_0=E-E_k$ and from the term with $\Lambda_-^{(1)}$ at $k_0=-E-E_k$. The state where particle 1 has ρ spin $+$ and particle 2 has $-$ (the $+-$ state) is absent since this has no poles in the upper half-plane, whereas the $-+$ state is absent due to a cancellation between the contributions from the first and second pole. A similar expression is found for the second term in Eq. (B14). The BSLT propagator is given by

$$\begin{aligned} S^{\mathrm{BSLT}}(p,P)&=\frac{1}{2}(E_p-E)\,\delta(p_0)S^{(1)}(p,P)S^{(2)}(p,P) \\ &=\frac{\Lambda_+^{(1)}(\mathbf{k})\Lambda_+^{(2)}(\mathbf{k})}{2(E_k-E)}-\frac{\Lambda_+^{(1)}(\mathbf{k})\Lambda_-^{(2)}(\mathbf{k})}{2(E_k+E)} \\ &\quad-\frac{\Lambda_-^{(1)}(\mathbf{k})\Lambda_+^{(2)}(\mathbf{k})}{2(E_k+E)}+\frac{\Lambda_-^{(1)}(\mathbf{k})\Lambda_-^{(2)}(\mathbf{k})}{2(E_k+E)}\,\frac{E_k-E}{E_k+E}. \end{aligned} \tag{B16}$$

Therefore, if we retain only the positive-energy contributions in both the expression for the current and in the evaluation of the T matrix, the current is conserved.

APPENDIX C: DETAILS OF THE INTEGRATION

In the discussion of the rescattering diagram it was seen that in the equal-time approximation the integration over the zeroth component of the relative internal momentum k can be done analytically. The resulting amplitude contains three terms, from each of the internal nucleons being on-shell. The remaining integral over the the relative three momentum $\mathbf{k}$ is calculated numerically. However, some of the terms have poles due to a second internal nucleon being on-shell. In this appendix we discuss how these poles were evaluated. The basic assumption in the following is that these poles are sufficiently far apart to be treated independently, which in the actual calculations turned out to be the case. A convenient choice is to have the photon momentum define the z direction, since then the poles only appear in the integration over θ and k.

When both nucleons are on-shell before emission of the photon a pole occurs when $E-E_k=0$, i.e., $k=p$. In this case the integration over θ and ϕ is straightforward, and the remaining integration is of the form

$$\mathcal{I}=\int_\alpha^\beta dkf(k)\,\frac{1}{E_k-E-i\varepsilon}, \tag{C1}$$

with $E_k=\sqrt{k^2+M^2}$. If the pole is in the interval (α,β), this can be rewritten in terms of a principal value integral plus a residue at the pole. In the principal value integral the value of the function at the pole can be subtracted. Then the integral $\mathcal{I}$ can be written as

$$\begin{aligned} \mathcal{I}=\mathcal{P}\int dk\frac{f(k)(E_k+E)-2f(p)E}{k^2-p^2}+2Ef(p)\mathcal{P}\int dk\frac{1}{k^2-p^2} \\ +i\pi f(p)\frac{E}{p}. \end{aligned} \tag{C2}$$

The first integral can be calculated numerically, since it is completely regular on the interval α,β. The second term in Eq. (C2) can be evaluated analytically,

$$\begin{aligned} \mathcal{I}_2&=2Ef(p)\mathcal{P}\int dk\frac{1}{k^2-p^2} \\ &=f(p)\frac{E}{p}\,\mathcal{P}\int dk\left(\frac{1}{k-p}-\frac{1}{k+p}\right). \end{aligned} \tag{C3}$$

The first integral yields

$$\lim_{\delta\downarrow 0}\left[\int_{\alpha}^{p-\delta}\frac{dk}{k-p}+\int_{p+\delta}^{\beta}\frac{dk}{k-p}\right]$$
$$=\lim_{\delta\downarrow 0}[\ln|k-p|_{\alpha}^{p-\delta}+\ln|k-p|_{p+\delta}^{\beta}]$$
$$=\lim_{\delta\downarrow 0}\ln\left(\frac{\delta(\beta-p)}{\delta(p-\alpha)}\right)=\ln\left(\frac{\beta-p}{p-\alpha}\right) \tag{C4}$$

and the second gives

$$\lim_{\delta\downarrow 0}\left[\int_{\alpha}^{p-\delta}\frac{dk}{k+p}+\int_{p+\delta}^{\beta}\frac{dk}{k+p}\right]$$
$$=\lim_{\delta\downarrow 0}[\ln|k+p|_{\alpha}^{p-\delta}+\ln|k+p|_{p+\delta}^{\beta}]$$
$$=\lim_{\delta\downarrow 0}\ln\left(\frac{(2p-\delta)(p+\beta)}{(p+\alpha)(2p+\delta)}\right)=\ln\left(\frac{\beta+p}{p+\alpha}\right). \tag{C5}$$

The final result for $\mathcal{I}_2$ is given by the subtraction of Eqs. (C4) and (C5),

$$\mathcal{I}_2=f(p)\frac{E}{p}\ln\left(\frac{(\beta-p)(p+\alpha)}{(p+\beta)(p-\alpha)}\right), \tag{C6}$$

which reduces to zero for $\alpha\downarrow 0$ and $\beta\rightarrow\infty$. However, in case of a general interval (α,β) this term does not vanish.

The other possible pole occurs when both nucleons in the integral are on-shell after the photon is emitted, that is when

$$2E-q-E_k-E_{\mathbf{k-q}}=0, \tag{C7}$$

with $E_{\mathbf{k-q}}=\sqrt{E_k^2-2kqx}$ and $x=\cos\theta$. Solving Eq. (C7) for x one finds

$$x_p=\frac{E_k(2E-q)-2E(E-q)}{kq}. \tag{C8}$$

If x_p lays in the interval $[-1,1]$ a pole in the integration over θ occurs, and the integrand can be written as a quotient of two functions f and g such that $f(x)$ is regular and $g(x)$ has a single pole at $x=x_p$. Then the integration over x is

$$\int_{-1}^{1}dx\frac{f(x)}{g(x)}=\mathcal{P}\int_{-1}^{1}dx\,\frac{f(x)}{g(x)}+i\pi\left[(x-x_p)\,\frac{f(x)}{g(x)}\right]_{x=x_p}. \tag{C9}$$

To find the residue numerically it is useful to rewrite g in such a way that the pole structure becomes apparent by multiplying both numerator and denominator with $2E-q-E_k-E_{\mathbf{k-q}}$,

$$g(x)=2E-q-E_k-\sqrt{E_k^2+q^2-2kqx}$$
$$=2kq\frac{x-x_p}{2E-q-E_k+\sqrt{E_k^2+q^2-2kqx}}, \tag{C10}$$

so that the residue is

$$\text{Res}=\frac{f(x_p)(2E-q-E_k+\sqrt{E_k^2+q^2-2kqx_p})}{2kq}$$
$$=\frac{f(x_p)(2E-q-E_k)}{kq}, \tag{C11}$$

where we have used that the pole occurs when Eq. (C7) is satisfied, so when $\sqrt{E_k^2+q^2-2kqx_p}=2E-q-E_k$. For purpose of numerical accuracy again a subtraction is applied in the principal value integral, and defining the nonsingular part of the integrand as $h(x)=(x-x_p)f(x)/g(x)$ the result is

$$\int_{-1}^{1}dx\frac{h(x)}{x-x_p}=\int_{-1}^{1}dx\frac{h(x)-h(x_p)}{x-x_p}+h(x_p)\ln\left|\frac{1-x_p}{1+x_p}\right|$$
$$+i\pi h(x_p). \tag{C12}$$

The result of the integral over θ can have logarithmic poles in k. These occur at the values of k for which

$$2E-q-\sqrt{k^2+m^2}-\sqrt{k^2+m^2+q^2\pm 2kq}=0, \tag{C13}$$

that is, whenever $x_p=\pm 1$ since then the argument of the logarithm in Eq. (C12) is zero. The solutions of Eq. (C13) are

$$k_p^{\pm}=\pm\frac{1}{2}\left((2E-q)\sqrt{\frac{E^2-m^2-Eq}{E^2-Eq}}\pm q\right). \tag{C14}$$

A double pole can occur when $E^2-m^2-Eq=0$, but in actual calculations this turned out not to be a problem. In the neighborhood of the pole the integrand behaves as

$$I_k=f_p(k)\ln|k-k_p|+f_r(k), \tag{C15}$$

where $f_p(k)$ and $f_r(k)$ are regular functions in k. For such functions a simple Gaussian integration is not possible, and instead logarithmic Gaussian integration can be used, based on the fact that

$$\int_0^1 f(x)\ln(x)=\sum_{i=1}^{n}f(x_i)w_n(x_i)+E(n), \tag{C16}$$

where $w_n(x_i)$ are logarithmic Gaussian integration weights for points x_i, and $E(n)$ is the error made by restricting the summation to n terms. Thus one has to rewrite the integral over k as an integration with boundaries 0 and 1. Sufficiently far from the pole the logarithmic behavior of the integrand can be ignored. Therefore the logarithmic integration can be restricted to an interval $[a,k_p]$ for $k<k_p$ or $[k_p,a]$ for $k>k_p$ with a chosen such that the other poles (either the other logarithmic pole or the one from the $E=E_k$) are outside the integration interval, and the integrand can be written as

$$I_k=f_p(k)\ln\left|\frac{k-k_p}{a-k_p}\right|-f_p(k)\ln|b-k_p|+f_r(k)$$
$$=F_p(k(z))\ln(z)+F_r(k(z)) \tag{C17}$$

with $z=|(k-k_p)/(a-k_p)|\in[0,1]$. The functions $F_p(k(z))$ and $F_r(k(z))$ are regular on the integration interval, and the integration over the first term can be done using Eq. (C16), whereas the integration over the second term can be done analytically.

APPENDIX D: LOW-ENERGY THEOREM FOR PROTON-PROTON BREMSSTRAHLUNG

We will derive the low-energy theorem for bremsstrahlung of two spin-$\frac{1}{2}$ particles in correspondence with the original work of Low [17]. Consider the contributions in which particle 1 emits the photon; the extension to emission from both particle 1 and 2 is straightforward. The initial particle has four momentum p, the final particle has four momentum p' and the photon has four momentum q. The spectator particle has momenta $\tilde{p}$ and $\tilde{p}'$. There are three principal variables on which the T matrix depends. Here we choose them to be the invariant mass M_i^2 of the initial particle, the invariant mass M_f^2 of the final particle, and a third parameter $\nu = p_\nu \cdot \tilde{p} + p'_\nu \cdot \tilde{p}'$ where $p_\nu = p - q$, $p'_\nu = p'$ or $p_\nu = p$, $p'_\nu = p' + q$. Then the following relations hold:

$$M_i^2 = (p-q)^2 \approx m^2 - 2p\cdot q, \quad M_f^2 = (p'+q)^2 \approx m^2 + 2p'\cdot q,$$

and define $\nu_0 = p\cdot\tilde{p} + p'\cdot\tilde{p}'$. The matrix element for the emission from external lines is thus

$$\begin{aligned} M_\mu^{\mathrm{ext}} = \overline{u(p')}\bigg[e\left(\gamma_\mu + \frac{i\kappa}{2m}\sigma_{\mu\nu}q^\nu\right)\frac{\not{p}'+\not{q}+m}{2p'\cdot q} \\ \times T(M_f^2, m^2, \nu_0 + q\tilde{p}') - T(m^2, M_i^2, \nu_0 - q\tilde{p}) \\ \times \frac{\not{p}+\not{q}+m}{2p\cdot q} e \\ \times \left(\gamma_\mu + \frac{i\kappa}{2m}\sigma_{\mu\nu}q^\nu\right)\bigg] u(p). \end{aligned} \tag{D1}$$

The T matrices can be expanded around the on-shell value, which up to first order gives the on-shell values $T_0 = T(m^2, m^2, \nu_0)$ and derivatives in the arguments M_f^2, M_i^2, and ν (which in the rest will be denoted by T_1, T_2, and T_3, respectively)

$$T(M_f^2, m^2, \nu_f) = T_0 + 2p'\cdot q T_1 + q\tilde{p}' T_3,$$

$$T(m^2, M_i^2, \nu_i) = T_0 - 2p\cdot q T_1 - q\tilde{p} T_3.$$

The $\sigma_{\mu\nu}$ term can be evaluated with the on-shell propagator, and up to terms of second order in the photon momentum the current is given by

$$\begin{aligned} M_\mu^{\mathrm{ext}} = e\overline{u(p')}\bigg[\left(\gamma_\mu - \frac{ie\kappa}{2m}\sigma_{\mu\nu}q^\nu\right)\frac{\not{p}'+m}{2p'\cdot q}T_0 - T_0\frac{\not{p}+m}{2p\cdot q}\left(\gamma_\mu - \frac{ie\kappa}{2m}\sigma_{\mu\nu}q^\nu\right)\bigg]u(p) + e\overline{u(p')}[\gamma_\mu(\not{p}'+m)T_1 \\ + T_2(\not{p}+m)\gamma_\mu]u(p) + e\overline{u(p')}\left[\gamma_\mu(\not{p}'+m)\frac{q\tilde{p}'}{p'\cdot q}T_3 + T_3\frac{q\tilde{p}}{p\cdot q}(\not{p}+m)\gamma_\mu\right]u(p) + e\overline{u(p')} \\ \times\left[\gamma_\mu\frac{\not{q}}{2p'\cdot q}T_0 + T_0\frac{\not{q}}{2p\cdot q}\gamma_\mu\right]u(p) + \mathcal{O}(q). \end{aligned} \tag{D2}$$

To see whether the nuclear current is conserved if only external diagrams are included, one can contract the current in Eq. (D2) with the photon four momentum q^μ. The terms with $\sigma_{\mu\nu}q^\nu$ and $\not{q}$ are trivially zero, since the photon is real ($q^2=0$). The term with no derivatives $M_{\mu,0}$ gives also zero,

$$\begin{aligned} q^\mu M_{\mu,0} &= eq^\mu\overline{u(p')}\left[\gamma_\mu\frac{\not{p}'+m}{2p'\cdot q}T_0 - T_0\frac{\not{p}+m}{2p\cdot q}\gamma_\mu\right]u(p) \\ &= e\overline{u(p')}\left[\frac{2p'\cdot q}{2p'\cdot q}T_0 - T_0\frac{2p\cdot q}{2p\cdot q}\right]u(p) = 0, \end{aligned} \tag{D3}$$

where we used that $(\not{p}+m)\gamma_\mu u(p) = 2p_\mu u(p)$ and equivalently for $\overline{u(p')}$. The sum $M_{\mu,12}$ of the terms with derivatives in the off-shell direction, T_1 and T_2, gives

$$\begin{aligned} q^\mu M_{\mu,12} &= eq^\mu\overline{u(p')}[\gamma_\mu(\not{p}'+m)T_1 + T_2(\not{p}+m)\gamma_\mu]u(p) \\ &= 2eq^\mu\overline{u(p')}(p'_\mu T_1 + T_2 p_\mu)u(p), \end{aligned} \tag{D4}$$

which in general is nonzero. The term $M_{\mu,3}$ with the derivative in the on-shell direction T_3 is given by

$$\begin{aligned} q^\mu M_{\mu,3} &= eq^\mu\overline{u(p')}\bigg[\gamma_\mu\frac{\not{p}'+m}{2p'\cdot q}(q\tilde{p}')T_3 \\ &\quad + T_3(q\tilde{p})\frac{\not{p}+m}{2p\cdot q}\gamma_\mu\bigg]u(p) \\ &= eq^\mu\overline{u(p')}\left[\frac{2p_\mu}{2p'\cdot q}(q\tilde{p}')T_3 + T_3(q\tilde{p})\frac{2p_\mu}{2p\cdot q}\right]u(p) \\ &= q^\mu[e\overline{u(p')}(\tilde{p}'_\mu + \tilde{p}_\mu)T_3 u(p)]. \end{aligned} \tag{D5}$$

It is clear that in general the current is not conserved due to the terms with derivatives of the T matrix, unless additional terms are included,

$$M_\mu^{\mathrm{int}} = -e\overline{u(p')}[2p'_\mu T_1 + 2p_\mu T_2 + (\tilde{p}'_\mu + \tilde{p}_\mu)T_3]u(p), \tag{D6}$$

These terms can be interpreted as internal contributions. After inclusion of these internal diagrams only the derivative in the on-shell direction remains. It can be rewritten in terms of the momenta of particle 1 only, using $\widetilde{p}'_\mu = \partial\nu/\partial p'_\mu$. Thus we can define a differential operator [26],

$$D_\mu(p) = \left(\frac{q\widetilde{p}'}{p'\cdot q} p'_\mu - \widetilde{p}'_\mu \right) \frac{\partial}{\partial\nu} = \frac{p'_\mu}{p'\cdot q} q^\nu \frac{\partial}{\partial p'^\nu} - \frac{\partial}{\partial p'^\mu}. \tag{D7}$$

With this operator the conserved current for bremsstrahlung can be written as

$$\begin{aligned} M_\mu = e\overline{u}(p') \Bigg[& \left(\frac{p'_\mu}{2p'\cdot q} T_0 - T_0 \frac{p_\mu}{2p\cdot q} \right) \\ & + \frac{i\kappa}{2m}\sigma_{\mu\nu}q^\nu \frac{\not{p}'+m}{2p'\cdot q} T_0 - T_0 \frac{\not{p}+m}{2p\cdot q} \frac{i\kappa}{2m}\sigma_{\mu\nu}q^\nu \Bigg] u(p) \\ & + e\overline{u}(p') \left[\frac{\gamma_\mu \not{q}}{2p'\cdot q} T_0 - T_0 \frac{\not{q}\gamma_\mu}{2p\cdot q} \right] u(p) \\ & + e\overline{u}(p') [\vec{D}_\mu(p') T + T \overleftarrow{D}_\mu(p)] u(p) + \mathcal{O}(q). \end{aligned} \tag{D8}$$

[1] F. de Jong, K. Nakayama, V. Herrmann, and O. Scholten, Phys. Lett. B **333**, 1 (1994).

[2] J. A. Eden and M. F. Gari, Phys. Rev. C **53**, 1102 (1996).

[3] F. de Jong and K. Nakayama, Phys. Lett. B **385**, 33 (1996).

[4] F. Gross, J. W. van Orden, and K. Holinde, Phys. Rev. C **45**, 2094 (1992).

[5] K. Michaelian *et al.*, Phys. Rev. D **41**, 2689 (1990).

[6] N. Kalantar, A. Bakker, H Huisman, J. G. Messchendorp, S. Schadmand, O. Scholten, and J. Zijlstra, Few-Body Syst., Suppl. **8**, 145 (1995).

[7] M. K. Liou, R. Timmermans, and B. F. Gibson, Phys. Lett. B **345**, 372 (1995); Phys. Rev. C **54**, 1574 (1996).

[8] J. Fleischer and J. A. Tjon, Nucl. Phys. **B84**, 375 (1974); Phys. Rev. D **15**, 2537 (1977); **21**, 87 (1980).

[9] M. J. Zuilhof and J. A. Tjon, Phys. Rev. C **24**, 736 (1980).

[10] E. E. van Faassen and J. A. Tjon, Phys. Rev. C **28**, 2354 (1983); **30**, 285 (1984).

[11] J. A. Tjon, Proceedings of the Les Houches Winterschool on Hadronic Physics with multi GeV electrons, Les Houches, 1990.

[12] R. Blankenbecler and R. Sugar, Phys. Rev. **142**, 1051 (1966); A. A. Logunov and A. N. Tavkhelidze, Nuovo Cimento **29**, 380 (1963).

[13] E. Hummel and J. A. Tjon, Phys. Rev. C **42**, 423 (1990); **49**, 21 (1994).

[14] R. A. Arndt, J. S. Hyslop, and L. D. Roper, Phys. Rev. D **35**, 128 (1987).

[15] G. H. Martinus, O. Scholten, and J. A. Tjon, Phys. Lett. B **402**, 7 (1997).

[16] S. Wallace, F. Gross, and J. A. Tjon, Phys. Rev. C **53**, 860 (1996).

[17] F. E. Low, Phys. Rev. **110**, 974 (1958).

[18] F. E. Low, Phys. Rev. **96**, 1428 (1954).

[19] S. J. Wallace, F. Gross, and J. A. Tjon, Phys. Rev. Lett. **74**, 228 (1995).

[20] V. Herrmann and K. Nakayama, Phys. Rev. C **46**, 2199 (1992).

[21] J. A. Eden and M. F. Gari, Z. Phys. A **347**, 145 (1993).

[22] M. Jetter and H. W. Fearing, Phys. Rev. C **51**, 1666 (1995).

[23] F. de Jong and K. Nakayama, Phys. Rev. C **52**, 2377 (1995).

[24] J. J. Kubis, Phys. Rev. D **6**, 547 (1972).

[25] J. D. Bjorken and S. D. Drell, *Relativistic Quantum Fields* (McGraw-Hill, New York, 1965).

[26] A. Yu. Korchin and O. Scholten, Nucl. Phys. **A581**, 439 (1995).